



Robotics 1

Robot components: Exteroceptive sensors

Prof. Alessandro De Luca

DIPARTIMENTO DI INGEGNERIA INFORMATICA
AUTOMATICA E GESTIONALE ANTONIO RUBERTI





Summary

- force sensors
 - strain gauges and joint torque sensor
 - 6D force/torque (F/T) sensor at robot wrist
 - RCC = Remote Center of Compliance (*not a sensor, but similar...*)
- proximity/distance sensors
 - infrared (IF)
 - ultrasound (US)
 - laser
 - with structured light
- vision
- examples of robot sensor equipments
- some **videos** intertwined, with applications

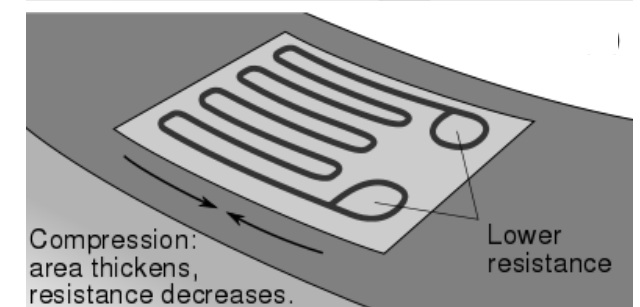
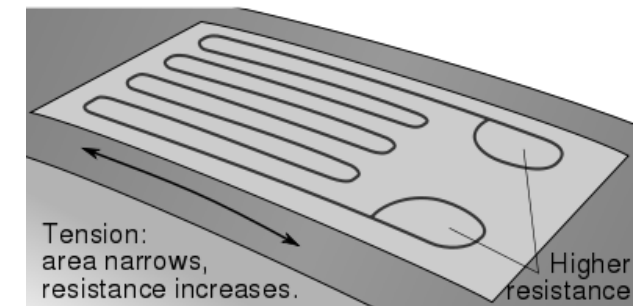
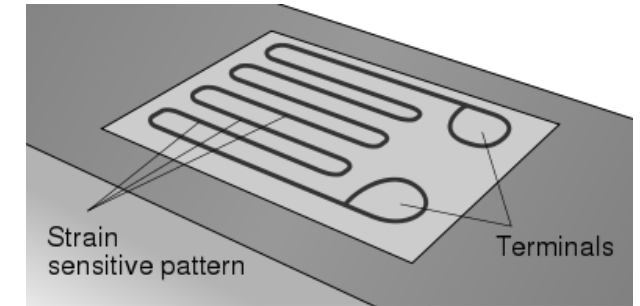


Force/torque and deformation

- indirect information obtained from the measure of **deformation** of an elastic element subject to the force or torque to be measured
- basic component is a *strain gauge*: uses the variation of the resistance R of a metal conductor when its length L or cross-section S vary

$$\frac{\partial R}{\partial L} > 0 \quad \frac{\partial R}{\partial S} < 0$$

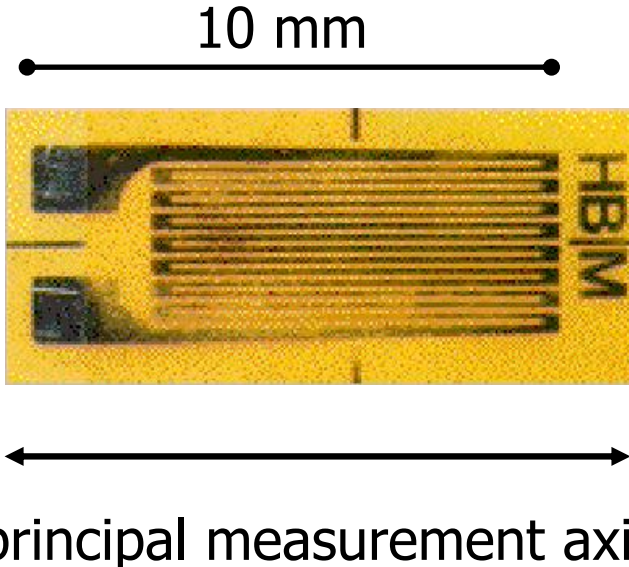
$\frac{\partial R}{\partial T}$ small



temperature



Strain gauges



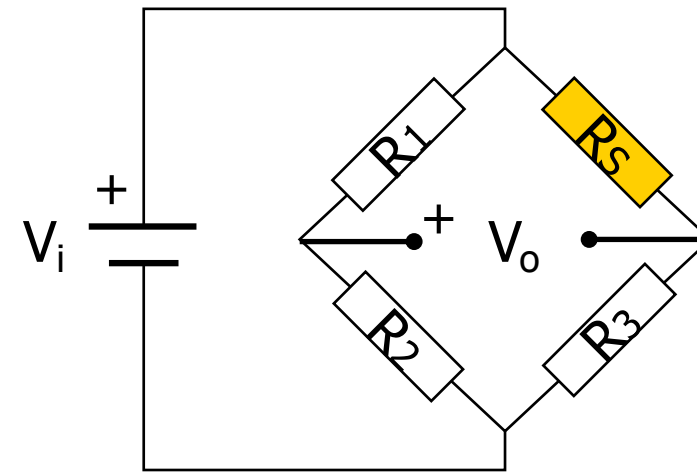
principal measurement axis

$$\text{Gauge-Factor} = \text{GF} = \frac{\Delta R/R}{\Delta L/L} \quad \text{strain } \varepsilon$$

(typically GF ≈ 2 , i.e., small sensitivity)

if R_1 has the same dependence on T of R_S
thermal variations are automatically
compensated

Wheatstone **single-point** bridge connection
(for *accurately* measuring resistance)



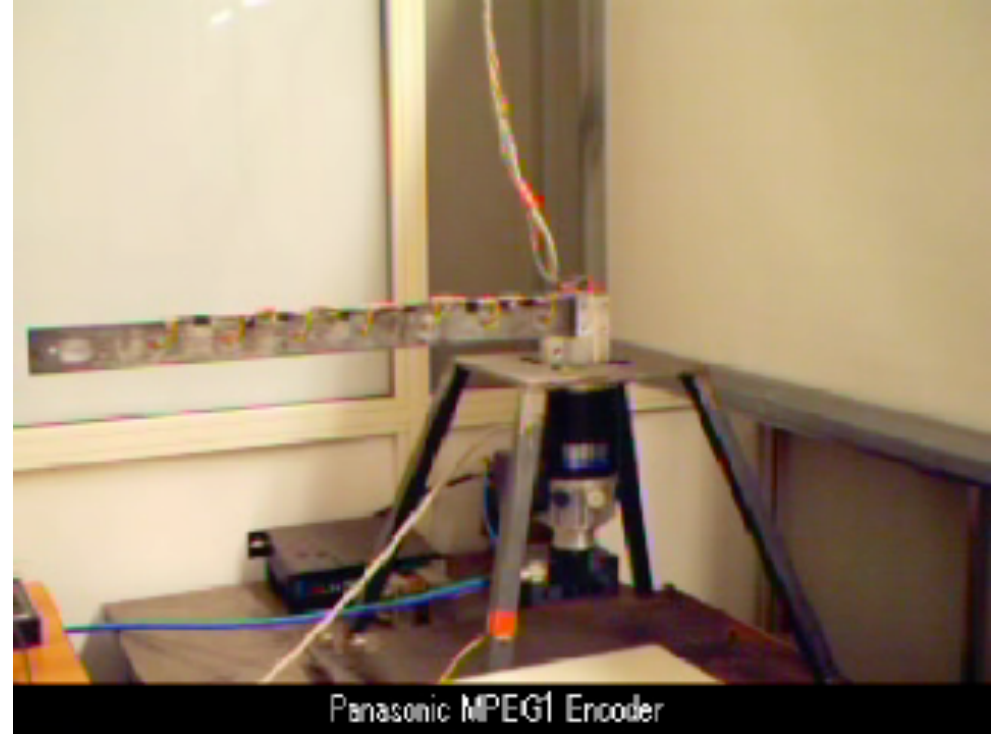
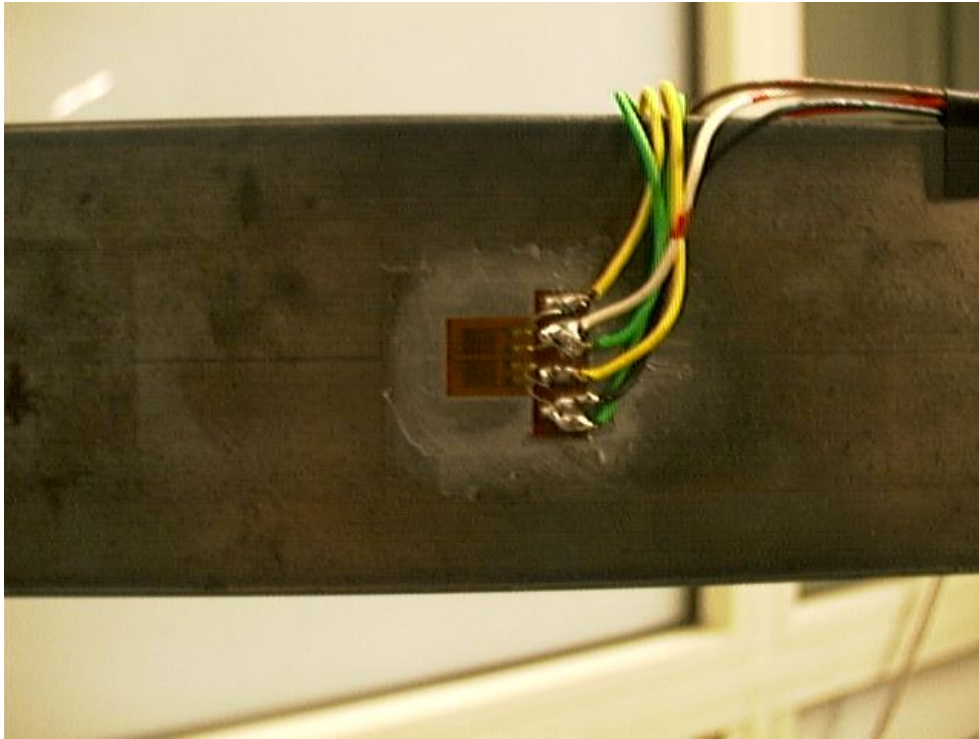
- R_1, R_2, R_3 very well matched ($\approx R$)
- $R_S \approx R$ at rest (no stress)
- **two-point** bridges have 2 strain gauges connected oppositely (\rightarrow sensitivity)

$$V_o = \left(\frac{R_2}{R_1+R_2} - \frac{R_3}{R_3+R_S} \right) V_i$$



Strain gauges in flexible arms

[video](#)

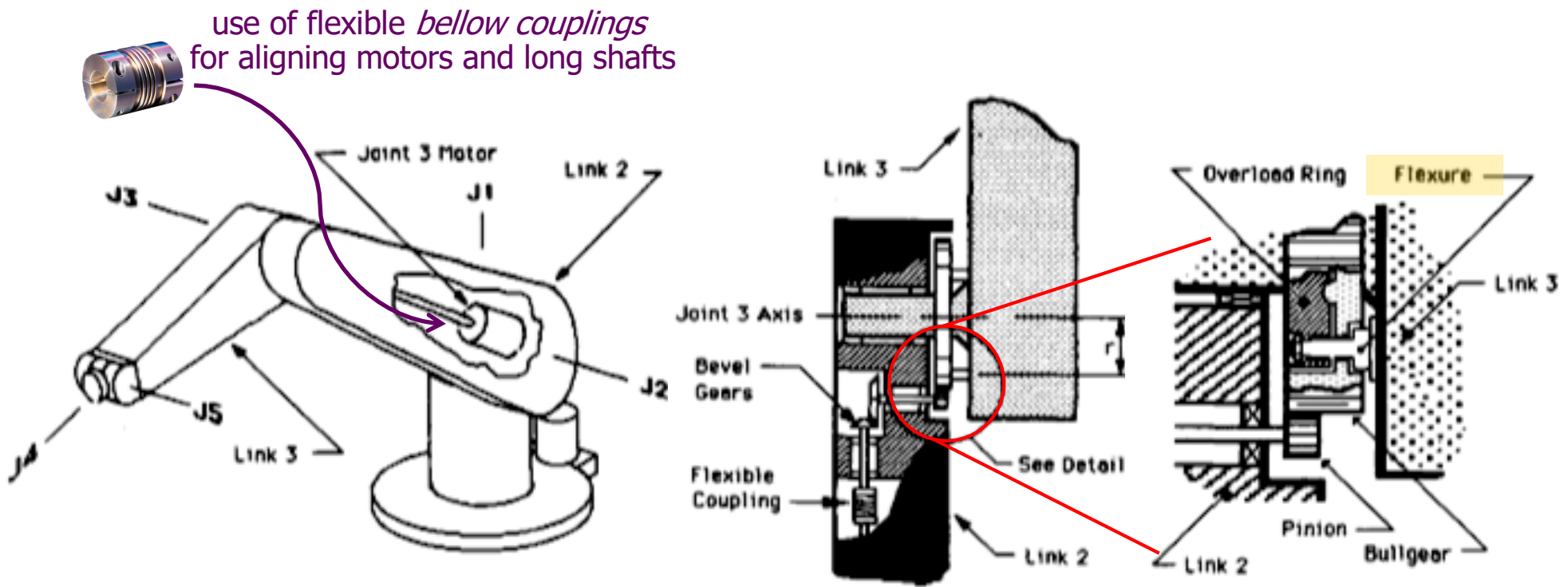


7 strain gauges glued⁽¹⁾ to a flexible aluminum beam (a robot “link”) measuring its local “curvature” in dynamic bending during slew motions (a **proprioceptive** use of these sensors)

⁽¹⁾ by cyanoacrylic glue



Torque sensor at robot joints



strain gauge mounted to “sense” the axial deformation
of the transmission shaft of joint #3 (elbow) in a PUMA 500 robot
(again, a **proprioceptive** use of this sensor)

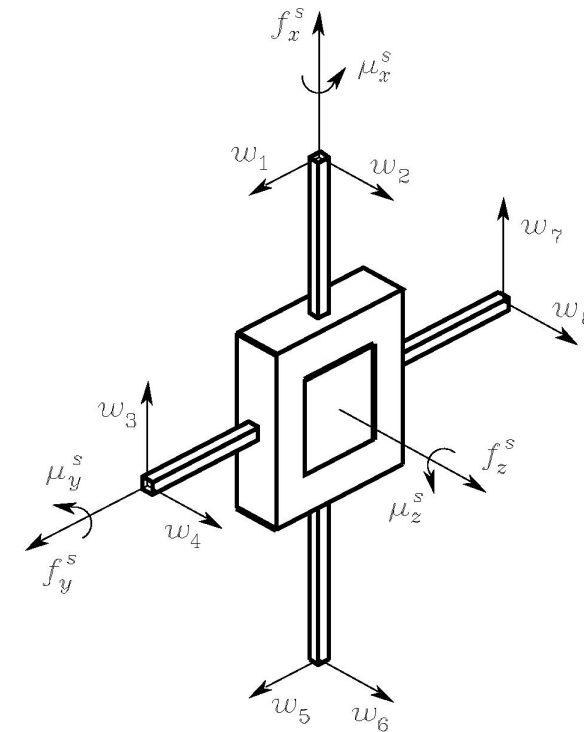
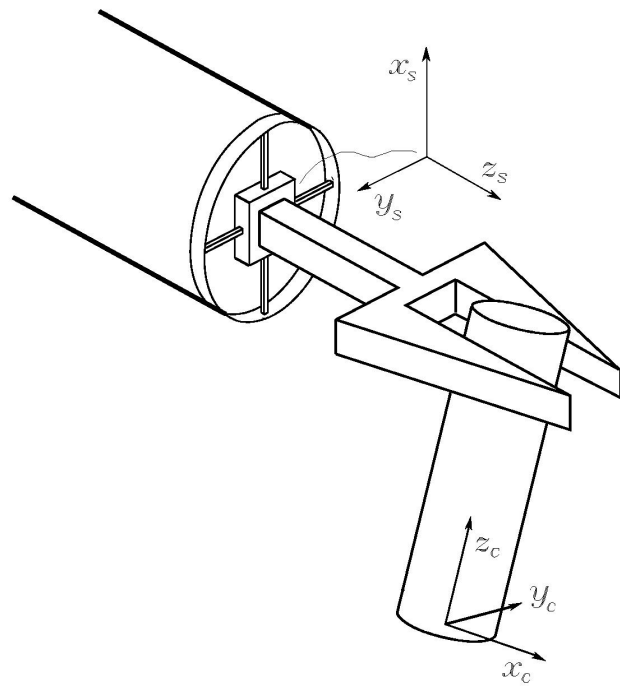


Force/torque sensor at robot wrist

- a device (with the outer form of a cylinder), typically located between the last robot link and its end-effector
- top and bottom plates are mechanically connected by a number of **deformable elements** subject to **strain** under the action of forces and moments
- there should be at least one such element in any direction along/around which a force or torque measure is needed
- since a complete “decoupling” of these measurements is hard to obtain, there are $N \geq 6$ such deformable elements
- on each element, a **pair of strain gauges** is glued so as to undergo opposite deformations (e.g., traction/compression) along the main axis of measurement



Maltese-cross configuration



- diameter ≈ 10 cm
- height ≈ 5 cm
- $50 \div 500$ N (resolution 0.1%)
- $5 \div 70$ Nm (resolution 0.05%)
- sample frequency ≈ 1 KHz

- 4 deformable elements
- two pairs of strain gauges are mounted on opposite sides of each element (8 pairs)
- the two gauges of each pair are placed adjacent on the same Wheatstone bridge



6D force/torque sensors

- ATI series
- cost (in 2016): about 6 K€ for Mini45 model + 700 € DAQ card

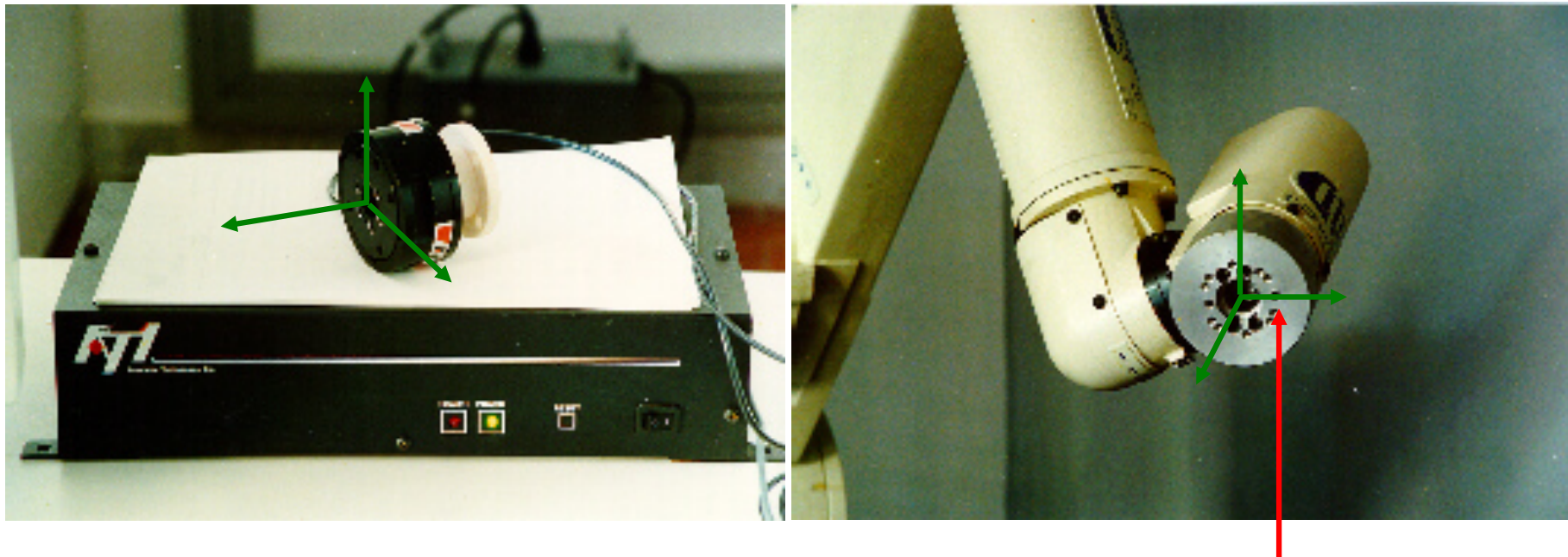


Model	Max Fx,Fy*	Max Tx,Ty*	Weight**	Diameter**	Height**
Nano17	±50 N	±500 N-mm	0.0091 kg	17 mm	14 mm
Nano25	±250 N	±6 N-m	0.064 kg	25 mm	22 mm
Nano43	±36 N	±500 N-mm	0.041 kg	43 mm	11 mm
Mini40	±80 N	±4 N-m	0.05 kg	40 mm	12 mm
Mini45	±580 N	±20 N-m	0.091 kg	45 mm	16 mm
Gamma	±130 N	±10 N-m	0.25 kg	75 mm	33 mm
Delta	±660 N	±60 N-m	0.91 kg	94 mm	33 mm
Theta	±2500 N	±400 N-m	5 kg	150 mm	61 mm
Omega160	±2500 N	±400 N-m	2.7 kg	160 mm	56 mm
Omega190	±7200 N	±1400 N-m	6.4 kg	190 mm	56 mm



6D force/torque sensor

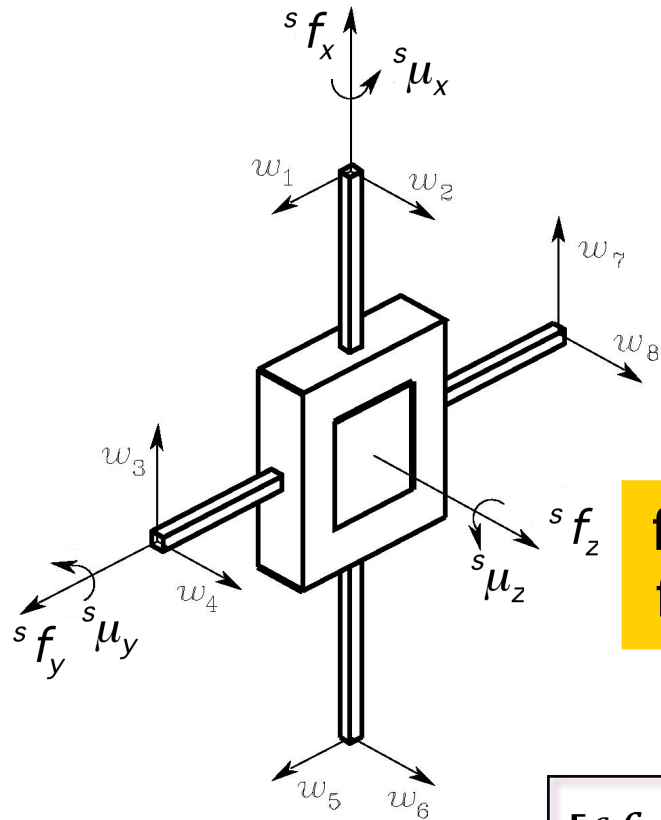
- electronic processing unit and mounting on an industrial robot (Comau Smart 3 robot, 6R kinematics)



mounting flange
(on link 6 of the manipulator arm)



6D F/T sensor calibration



$$\begin{bmatrix} {}^s f_x \\ {}^s f_y \\ {}^s f_z \\ {}^s \mu_x \\ {}^s \mu_y \\ {}^s \mu_z \end{bmatrix} = \begin{bmatrix} 0 & 0 & c_{13} & 0 & 0 & 0 & c_{17} & 0 \\ c_{21} & 0 & 0 & 0 & c_{25} & 0 & 0 & 0 \\ 0 & c_{32} & 0 & c_{34} & 0 & c_{36} & 0 & c_{38} \\ 0 & 0 & 0 & c_{44} & 0 & 0 & 0 & c_{48} \\ 0 & c_{52} & 0 & 0 & 0 & c_{56} & 0 & 0 \\ c_{61} & 0 & c_{63} & 0 & c_{65} & 0 & c_{67} & 0 \end{bmatrix} \begin{bmatrix} w_1 \\ w_2 \\ w_3 \\ w_4 \\ w_5 \\ w_6 \\ w_7 \\ w_8 \end{bmatrix}$$

force/torque measured in the frame attached to the sensor

calibration matrix

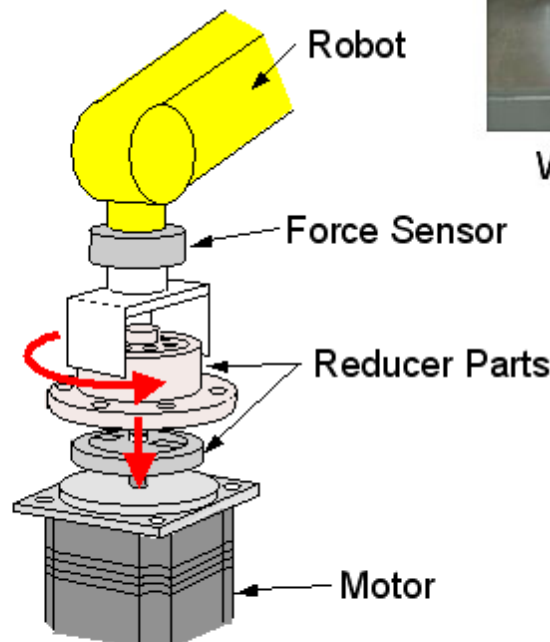
$$\begin{bmatrix} {}^c f_c \\ {}^c \mu_c \end{bmatrix} = \begin{bmatrix} {}^c R_s & 0 \\ S({}^c r_{cs}) {}^c R_s & {}^c R_s \end{bmatrix} \begin{bmatrix} {}^s f_s \\ {}^s \mu_s \end{bmatrix}$$

transformation from the sensor frame to the load/contact frame (at TCP)

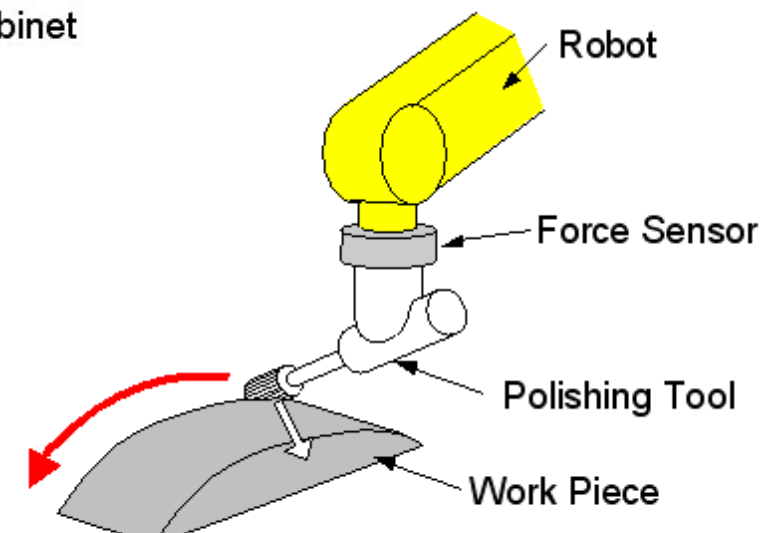
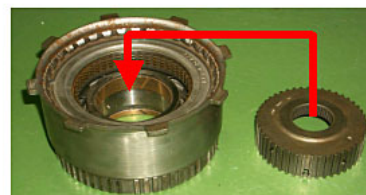
output of Wheatstone bridges



Typical uses of a F/T sensor



Phase matching by force sensing



Following with constant pushing force



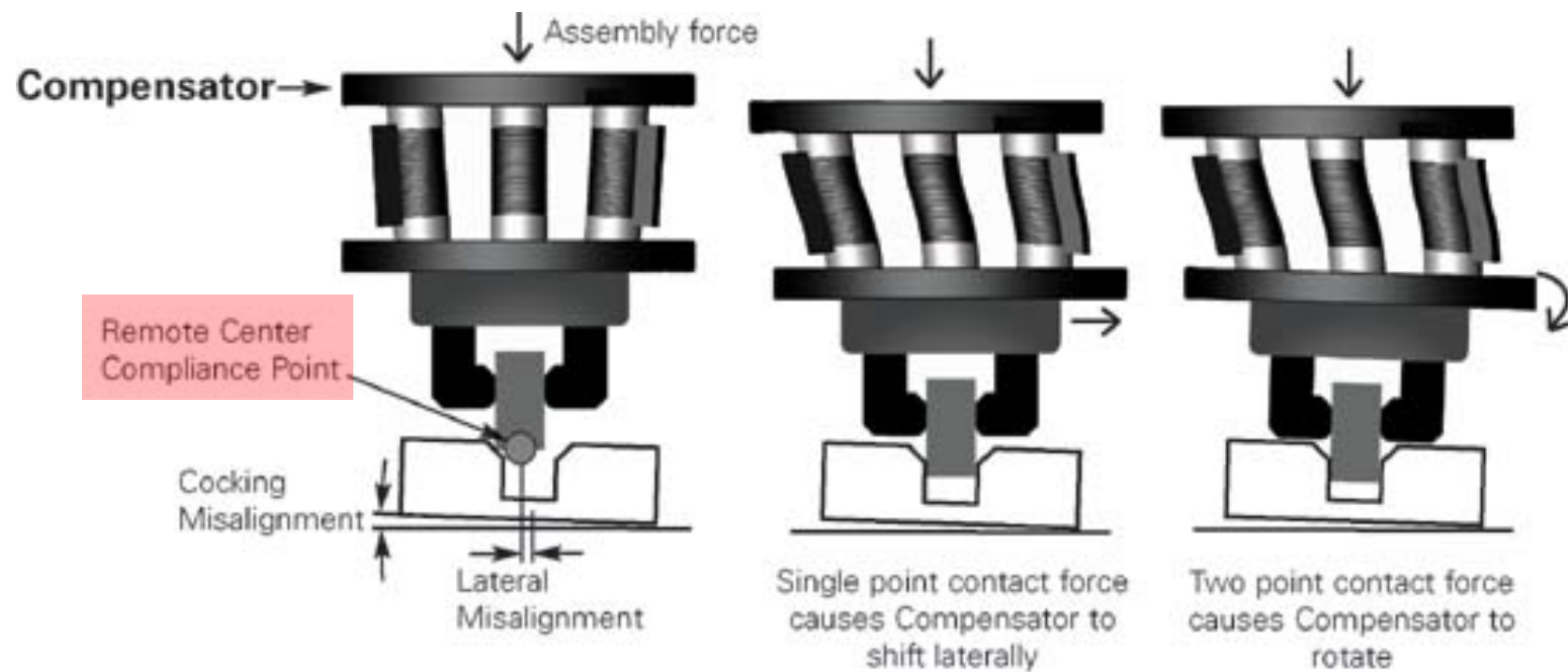
Passive RCC device

- RCC = Remote Center of Compliance
- placed on the wrist so as to introduce **passive “compliance”** to the robot end-effector, in response to static forces and moments applied from the environment at the contact area
- mechanical construction yields “**decoupled**” linear/angular motion responses **if** contact occurs at or near the RCC point



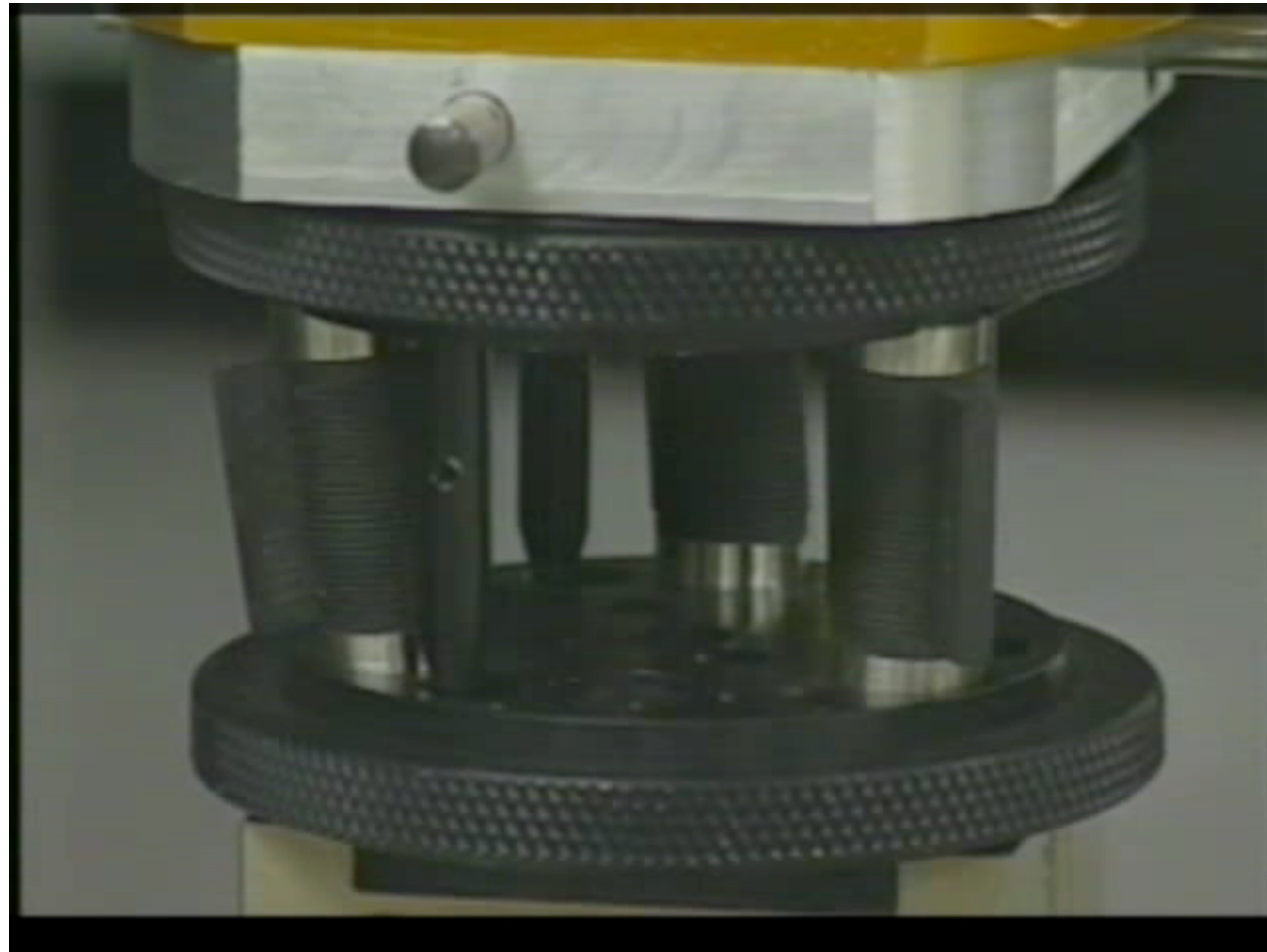


Assembly with RCC





Passive assembly with RCC



video

RCC by ATI Industrial Automation
<http://www.ati-ia.com>



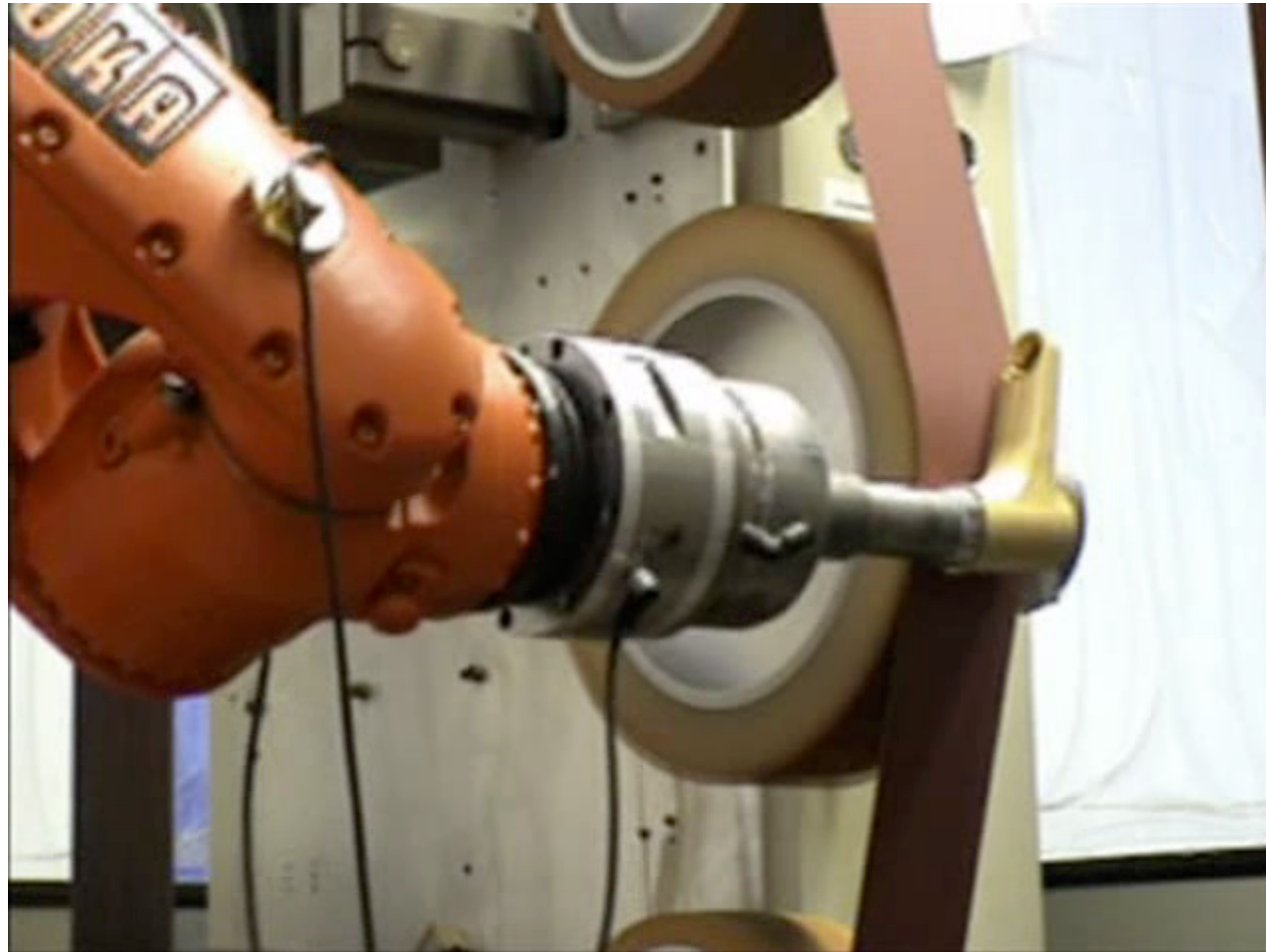
Active assembly with F/T sensor



ABB robot with ATI F/T sensor



Surface finishing with F/T sensor



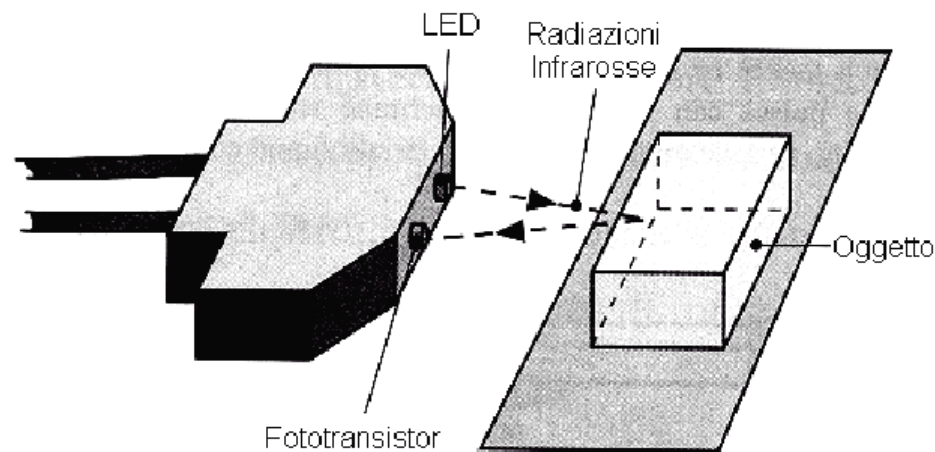
video

KUKA robot with F/T sensor



Proximity/distance sensors - 1

- **infrared:** a light source (LED) emitting a ray beam (at 850 ± 70 nm) which is then captured by a receiver (photo-transistor), after reflection by an object
- received intensity is related to distance
 - narrow emitting/receiving angle; use only indoor; reflectance varies with object color
- typical sensitive range: $4 \div 30$ cm or $20 \div 150$ cm
- cost: 15 €

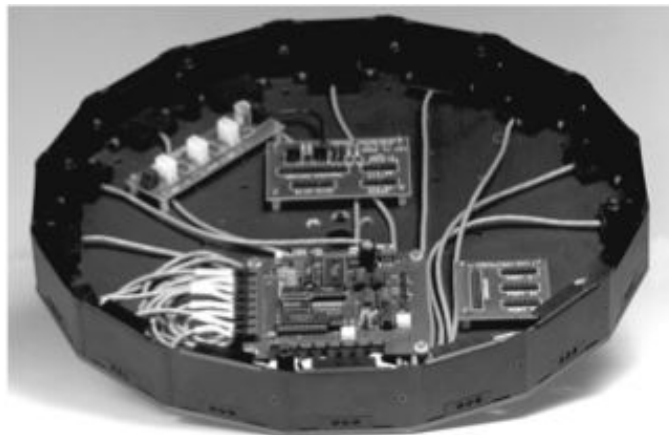


IR sensor SHARP GP2
(supply 5V, range $10 \div 80$ cm)



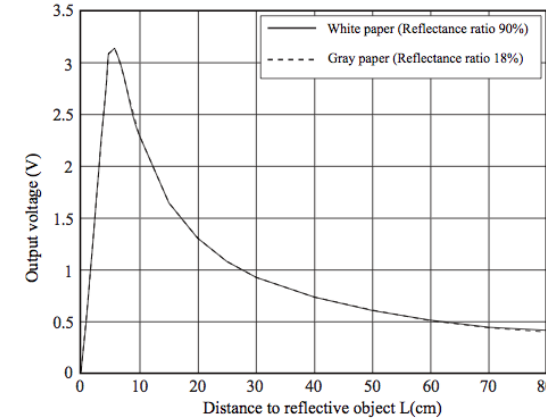
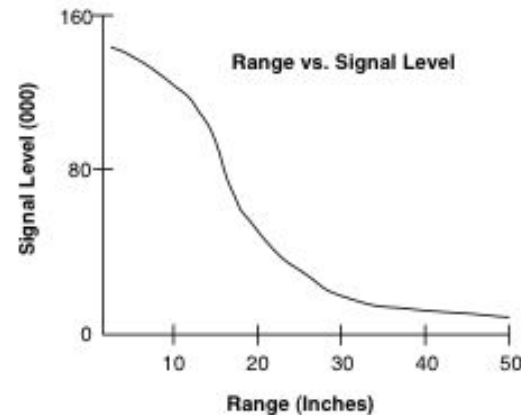
Infrared sensor

example: Sensus 300
on Nomad 200 mobile robot
(power data: 500 mA at 12 V)

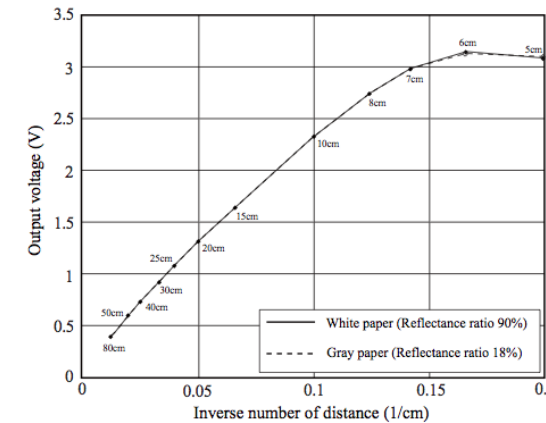


ring with 16 IR sensors

Sensus 300



Sharp GP2



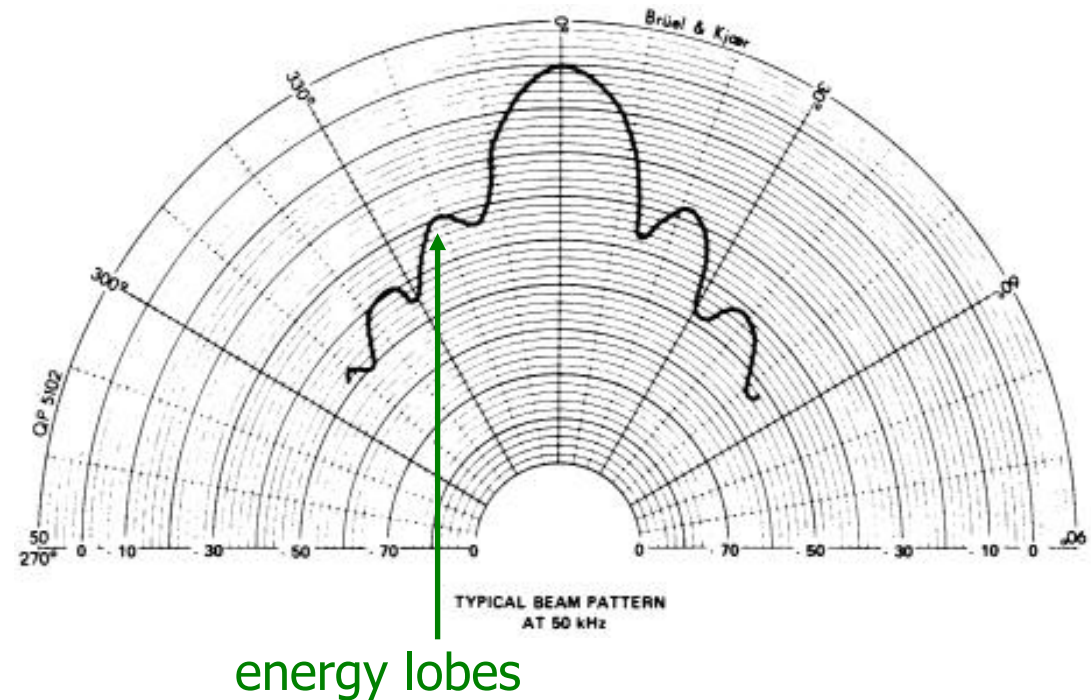
variation of received signal level as a direct or inverse function of distance



Proximity/distance sensors - 2

- **ultrasound:** use of sound wave propagation and reflection (at > 20 kHz, mostly 50 kHz), generated by a piezoelectric transducer excited by alternate voltage ($V \sin \omega t$)
- distance is proportional to the **Time-Of-Flight** (TOF) along the sensor-object-sensor path

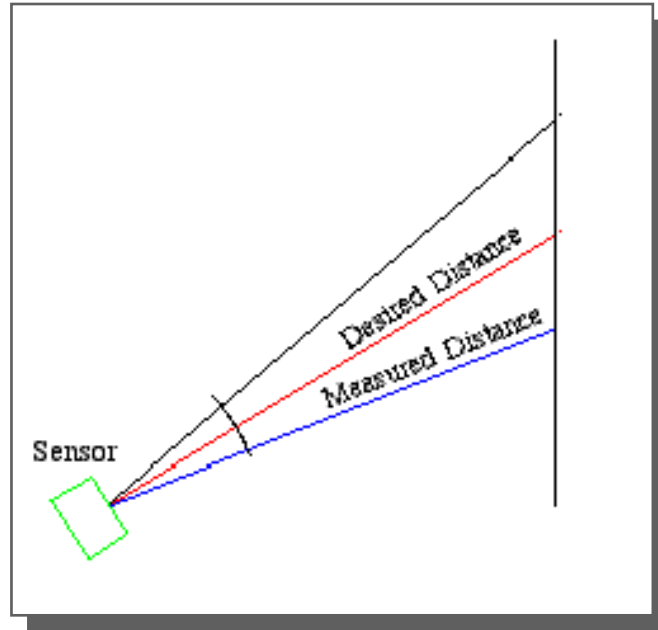
wave emitting angle $\approx 30^\circ$
allows to detect also obstacles located slightly aside from the front direction (but with uncertainty on their angular position)



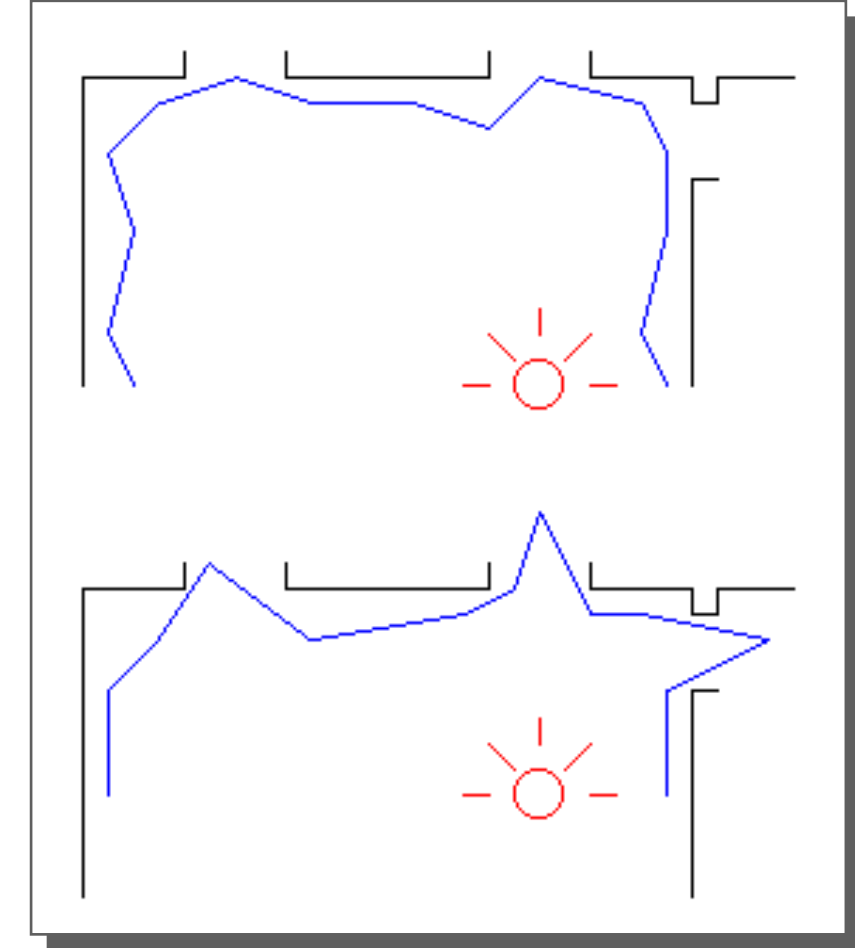


Ultrasound sensor

some problems related to US wave propagation

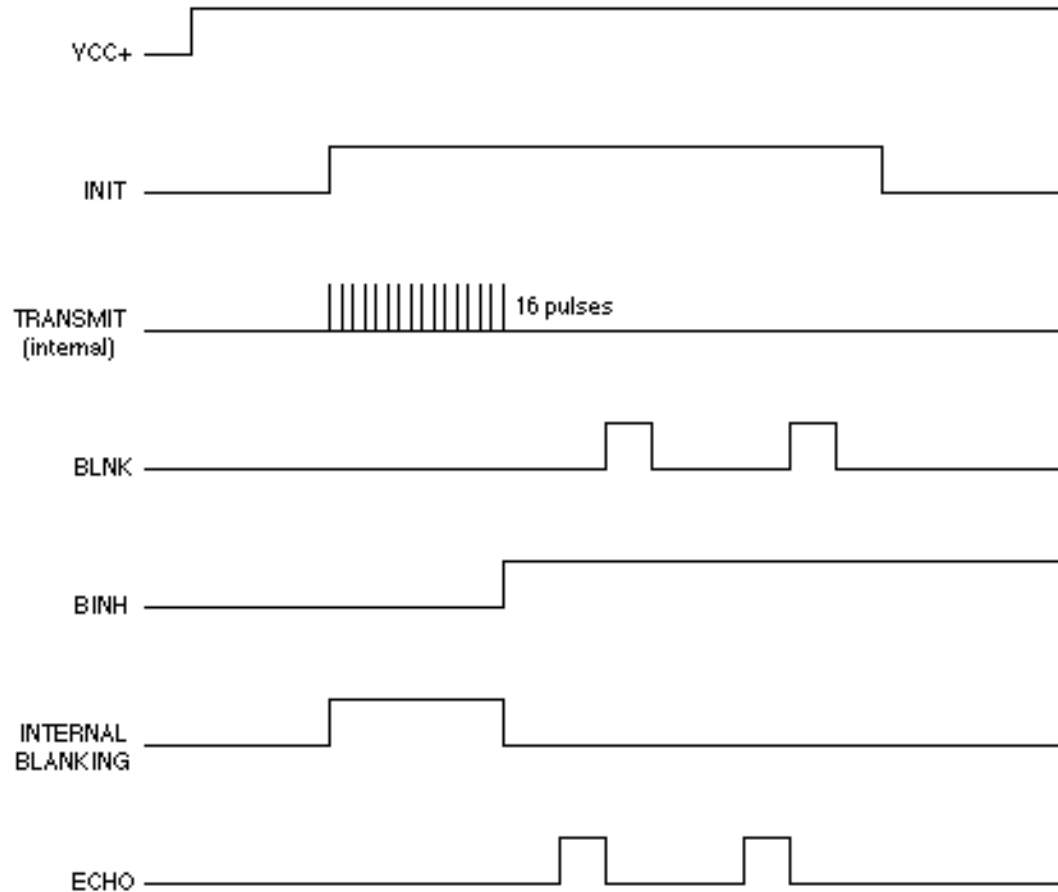


- uncertainty in distance evaluation within the cone of emission
- multiple reflections/echoes
- absorbing surfaces
- mirroring surfaces





Range limits for US sensors

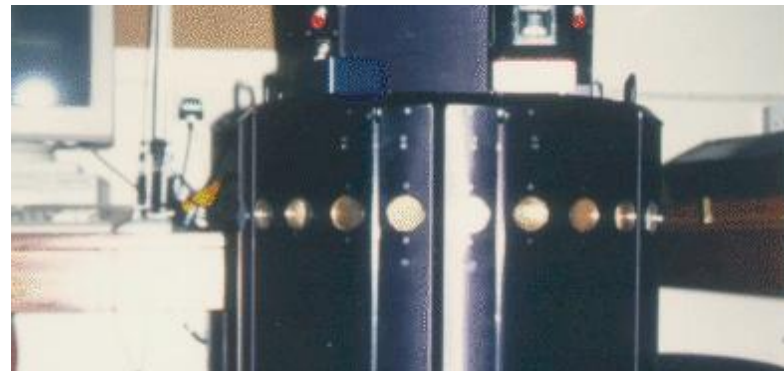


- during US pulses transmission the receiver is disabled, so as to avoid interferences that may lead to false readings
- the same is done after receiving the first echo, so as to avoid multiple reflections from the same object
- this limits the minimum distance that can be detected ($> 0.5 \text{ m}$)
- due to angular dispersion during emission, wave energy decreases with d^2
- to compensate for this effect, the gain of the receiver is increased over time (up to a limit)
- max detectable distance $\approx 6.5 \text{ m}$



Polaroid ultrasound sensor

- complete “kit” with trans-receiver and circuitry
- 3.5 ms of TOF for a front obstacle placed at 60 cm of distance
- range: 0.5÷2.5 m
- cost: < 30 €
- typical circular mounting of 16-32 US sensors (with a suitable sequence of activation)



Polaroid USP3

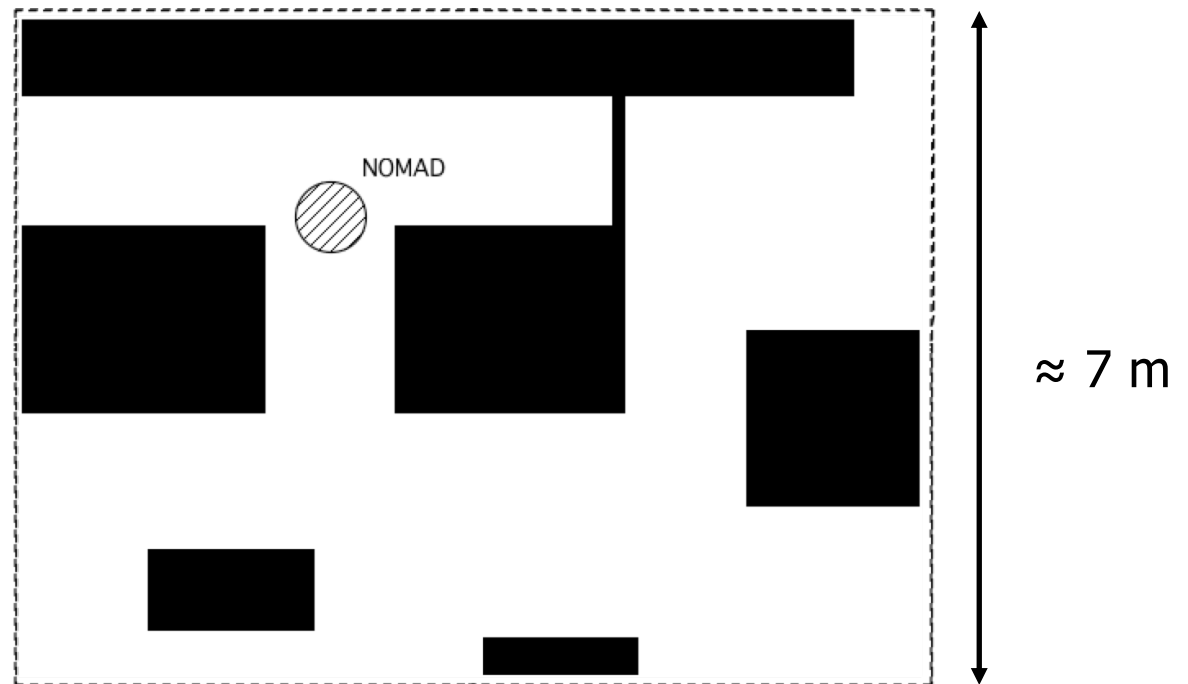
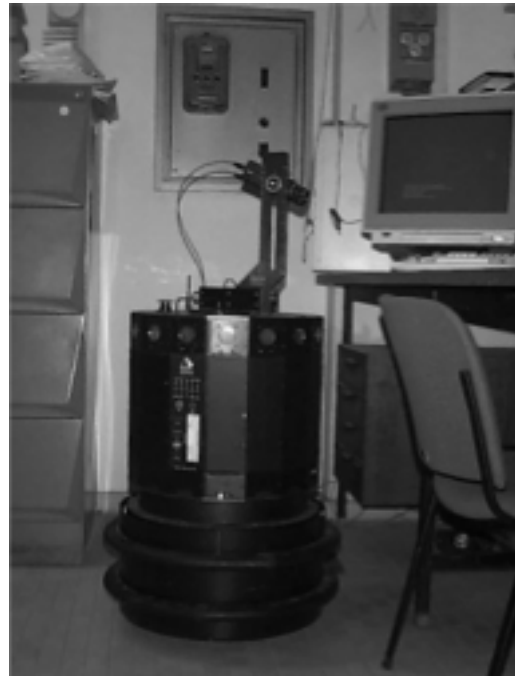


Migatron RPS 409



Navigation with ultrasound sensing

- Nomad 200 with 16 US sensors (plus other not used here)

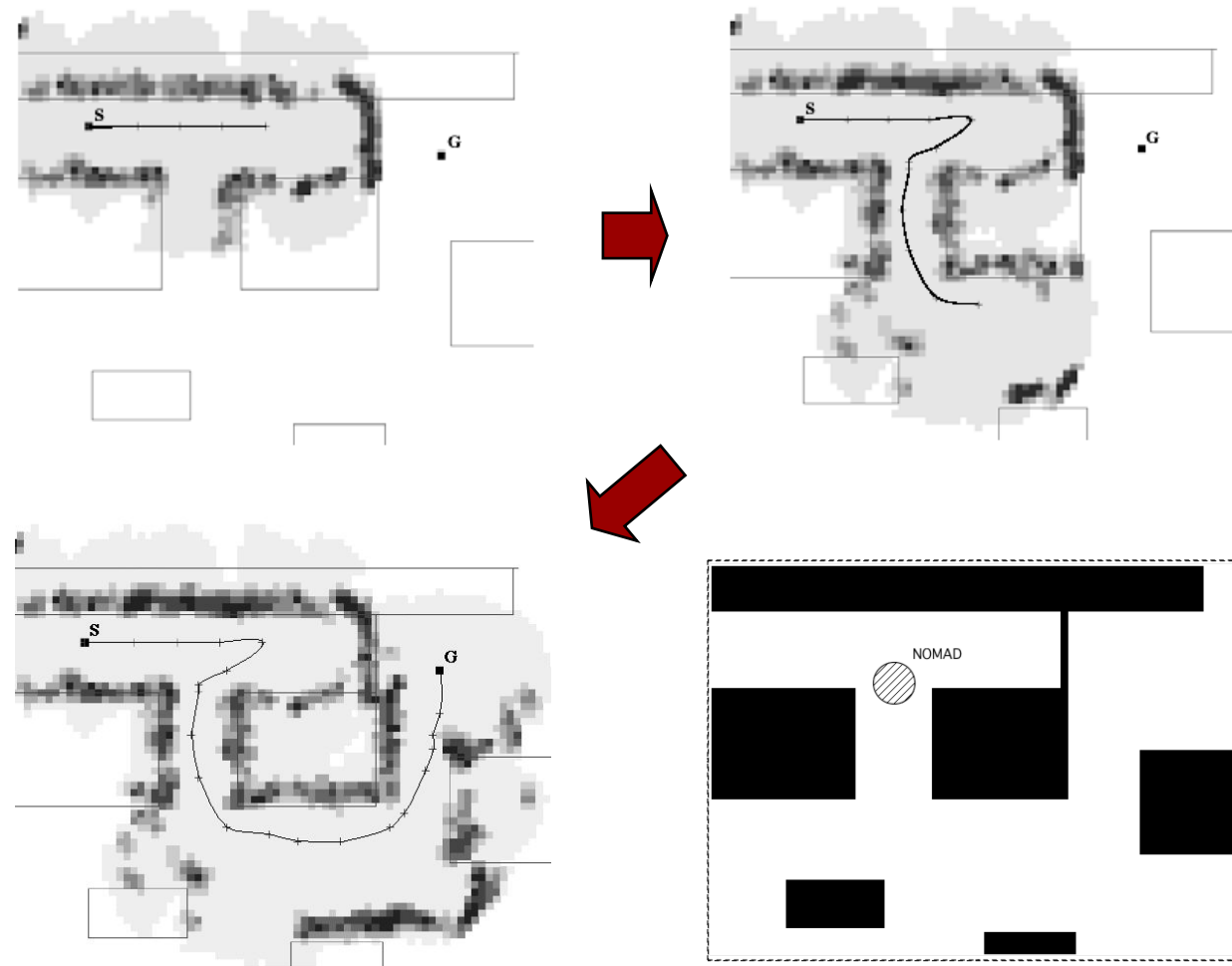


view of the robot and map of the former DIS Robotics Lab in Via Eudossiana 18
(the map is initially unknown to the robot)



Navigation with ultrasound sensing

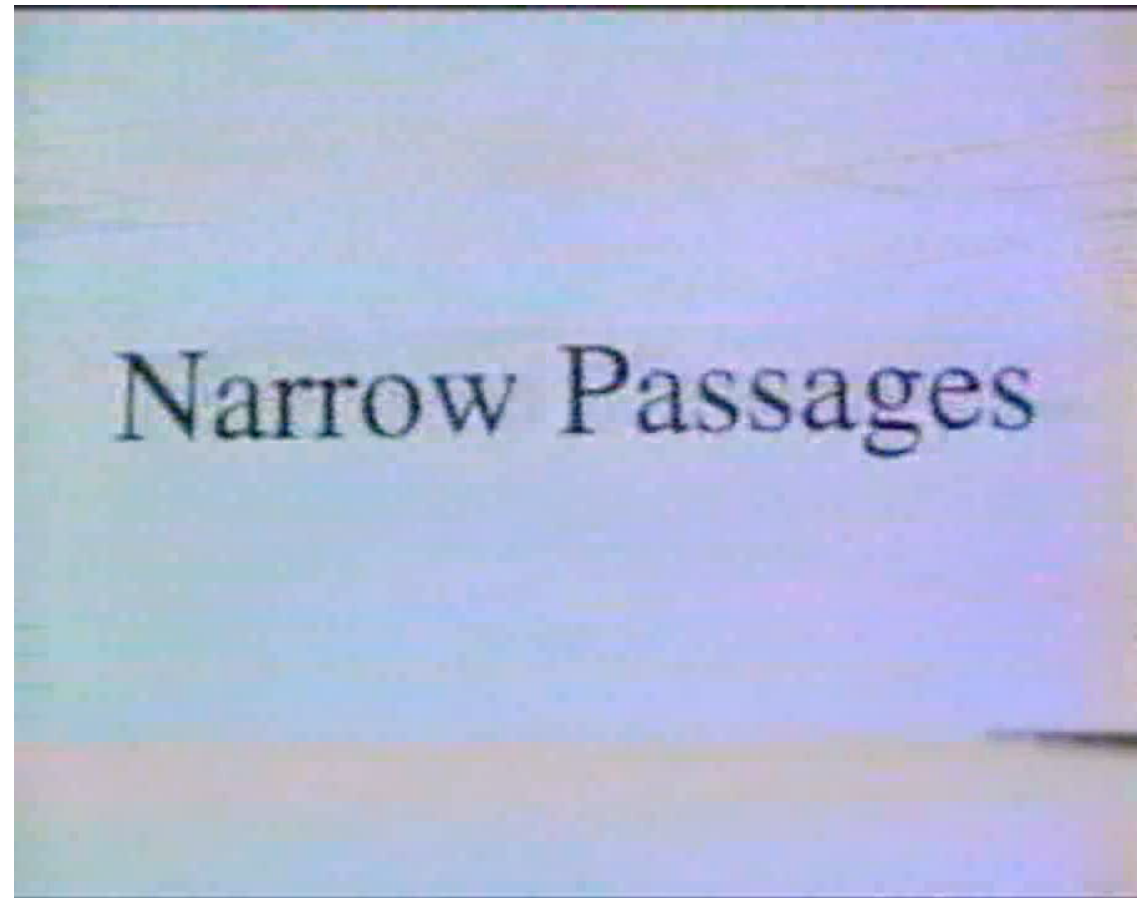
- grid map (unit = 10 cm) obtained by weighting successive data readings from US sensors with **fuzzy logic**; “aggressive” motion planning with **A*** search algorithm on graphs; **reactive** US-based navigation to avoid unexpected obstacles





Narrow passages

- Nomad 200 navigating with 16 ultrasonic sensors (old Robotics Lab, 1995)



video

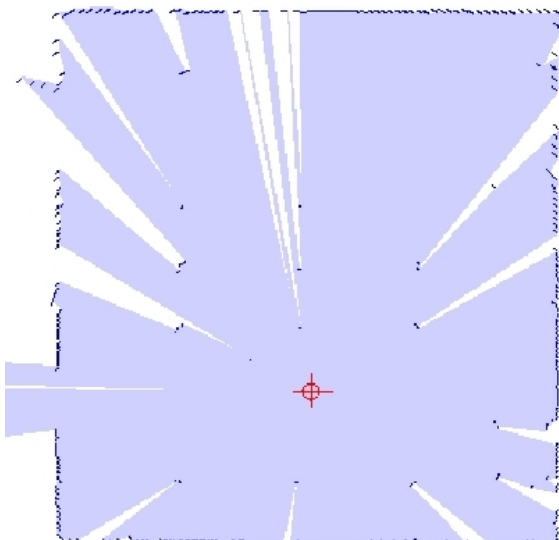


Proximity/distance sensors – 3

- **laser scanner:** two-dimensional scan of the environment with a radial field of **infrared** laser beams (laser radar)
 - time between transmission and reception is directly proportional to the distance to the object (**Time-of-Flight**)

■ **Sick LMS 200**

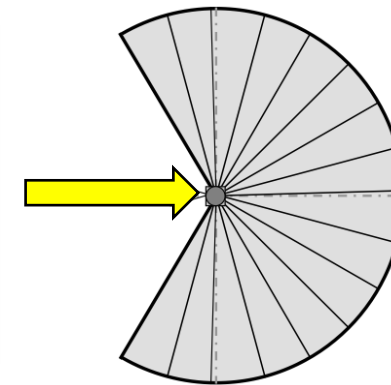
- wide angular range: max 180°
- high angular resolution that can be set by the user: $0.25^\circ - 0.5^\circ - 1^\circ$
- response time: 53 - 26 - 13 msec (depending on resolution)
- large range: 10 m up to $50 \div 80$ m
- depth resolution: ± 15 mm
- interface: RS-232, RS-422
- used to be quite expensive (about 5000 €, this model now discontinued)





A smaller laser scanner

- **Hokuyo URG-04X**
 - size: $50 \times 50 \times 70$ mm
 - weight: 160 g
 - angular range: max 240°
 - angular resolution: 0.36°
 - response: 100 msec/scan
 - range: 0.02 ÷ 4 m
 - depth resolution:
 - ± 1 cm (up to 1 m)
 - $\pm 1\%$ (beyond 1 m)
 - interface: RS-232, USB 2.0
 - supply: 5V DC
 - cost: 945 € (1080 US\$)
 - 2 years ago was 1750 € ...



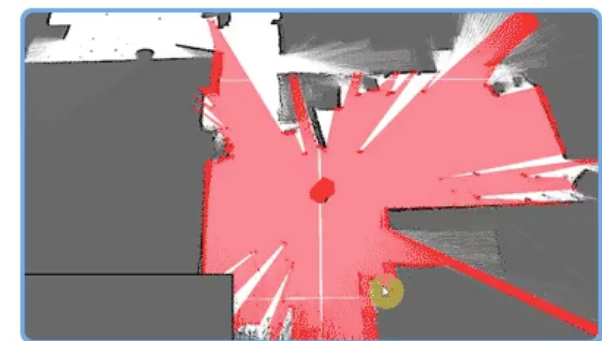
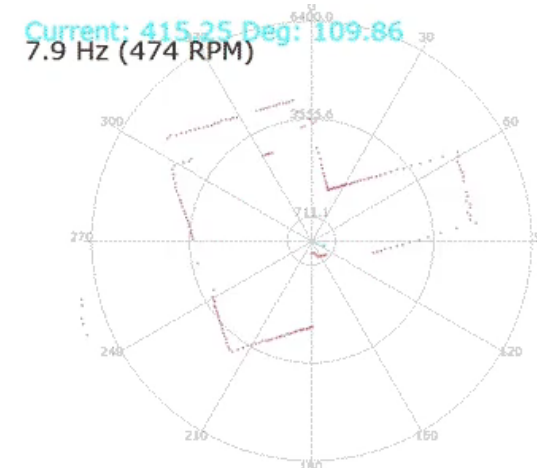
4 small Khepera with Hokuyo sensors
@ DIAG Robotics Lab



Rotating laser scanner

■ RoboPeak RPLidar A1M1

- 360° 2D-scan, 6 m measurement range
- size: 70 × 98.5 × 60 mm
- weight: 200 g
- variable scanning rate: 2 ÷ 10 Hz
 - by varying the motor PWM signal
- angular resolution: $\approx 1^\circ$ @5.5 Hz rate
 - 2000 samples/s @5.5 Hz rate
- depth resolution: ± 20 mm (0.2% of current depth)
- cost: 335 € (383 US\$) in development kit
- ROS & SLAM ready



Realtime ICP-SLAM based on RPLIDAR



Localization and mapping

- SLAM (Simultaneous Localization and Mapping) with a laser scanning sensor mounted on a mobile robot



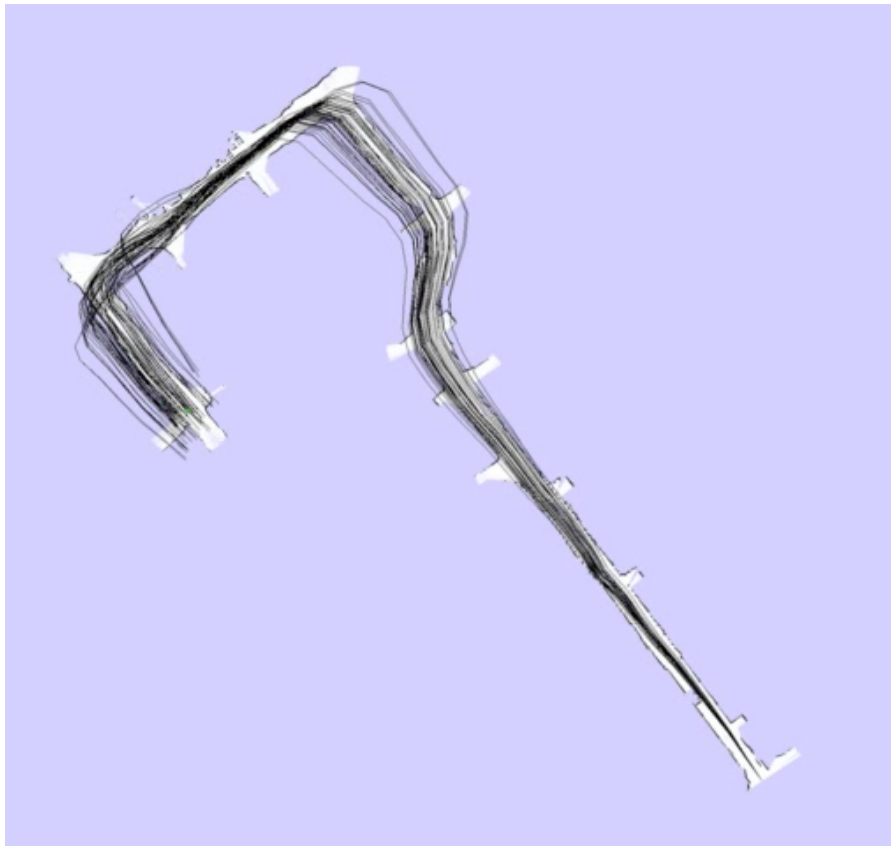
- An “extended” state estimation problem: determine at the same time
 - I. a map of the environment (sometimes, of its “landmarks” only)
 - II. the robot location within the mapusing an incremental, iterative measurement process (large scale data)



Localization and mapping

illustrating the benefit of “loop closure” on long range data (map correction)

video



single loop

video

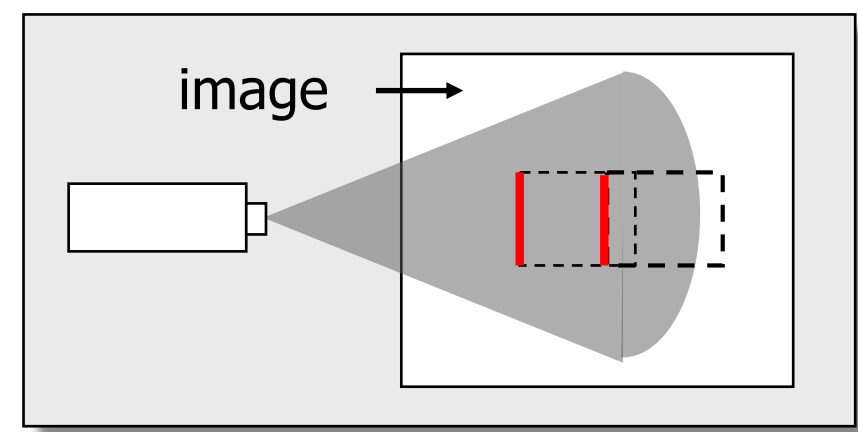
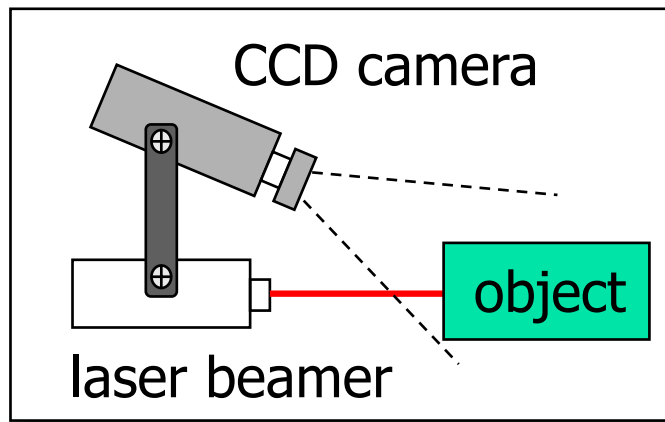


multiple loops (MIT Campus)

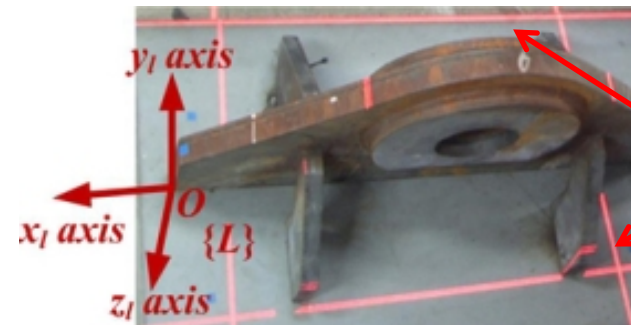


Proximity/distance sensors - 4

- **structured light:** a laser beam (coherent light source) is projected on the environment, and its planar intersection with surrounding objects is detected by a (tilted) camera
- the position of the “red pixels” on the camera image plane is in **trigonometric** relation with the object distance from the sensor



side view



top view

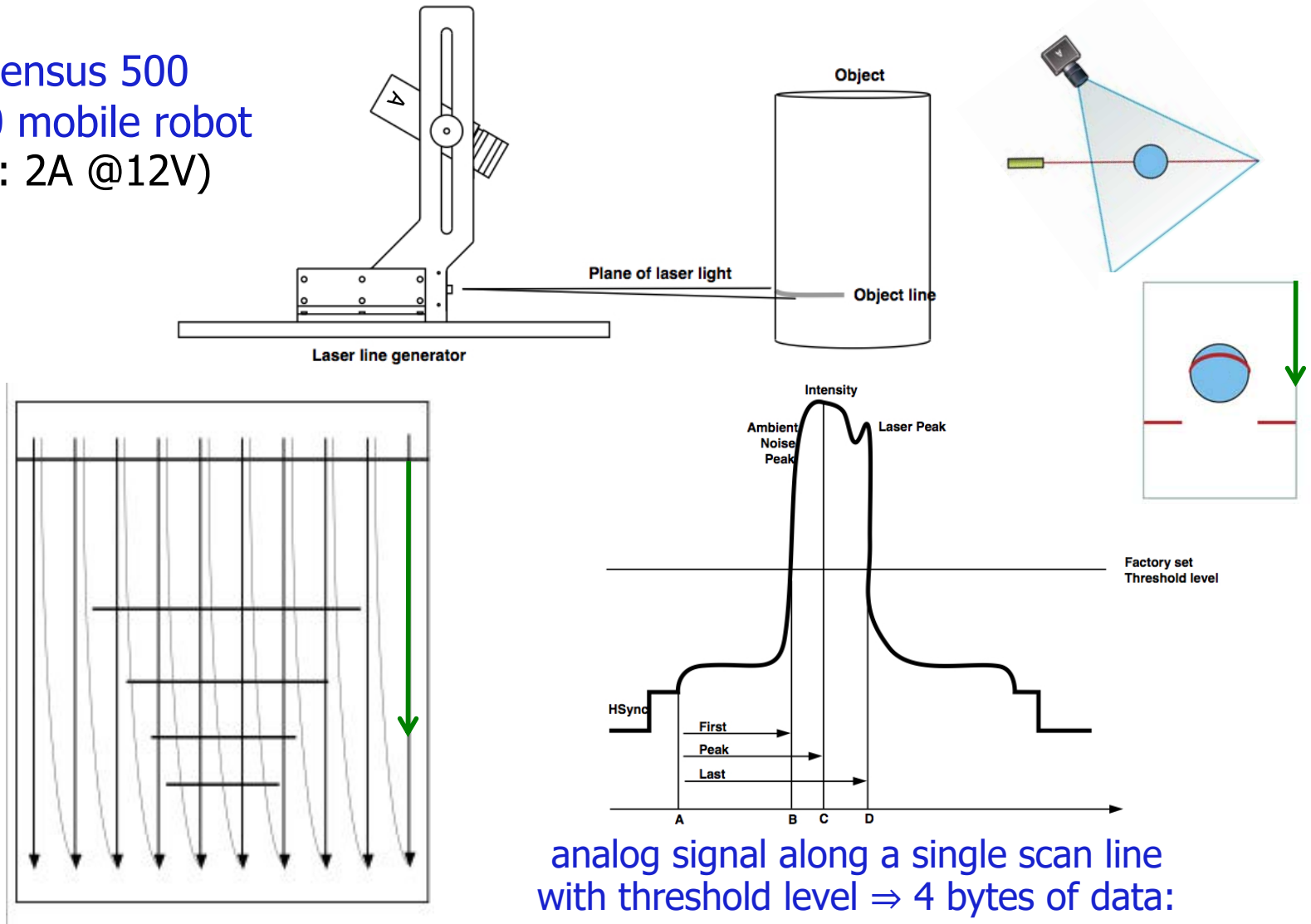
projected laser beams
(2D in this case)



Structured light sensor

example: Sensus 500
on Nomad 200 mobile robot
(power data: 2A @12V)

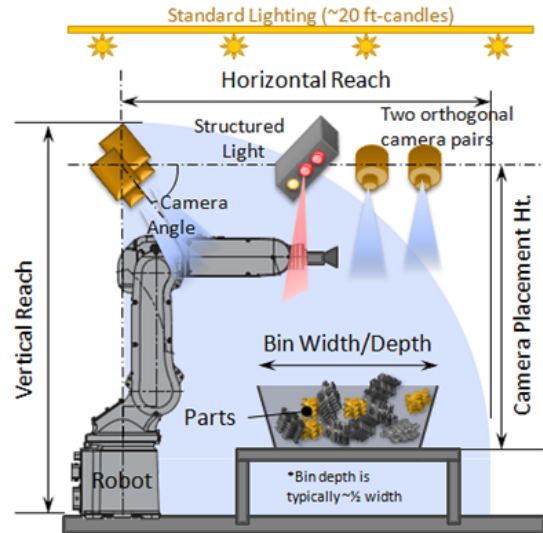
CCD camera with
 510×490 pixels
(rotated by 90°
with respect to the
480 scan lines)



analog signal along a single scan line
with threshold level \Rightarrow 4 bytes of data:
pixels FIRST, LAST, PEAK; value INTENSITY



Use of structured light sensors



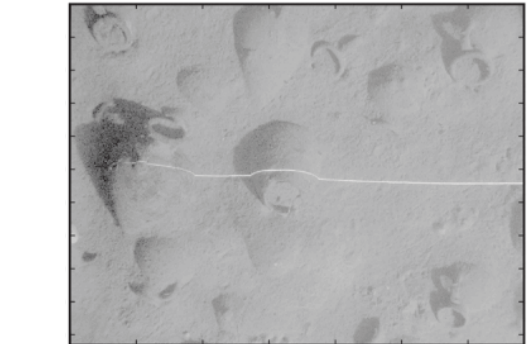
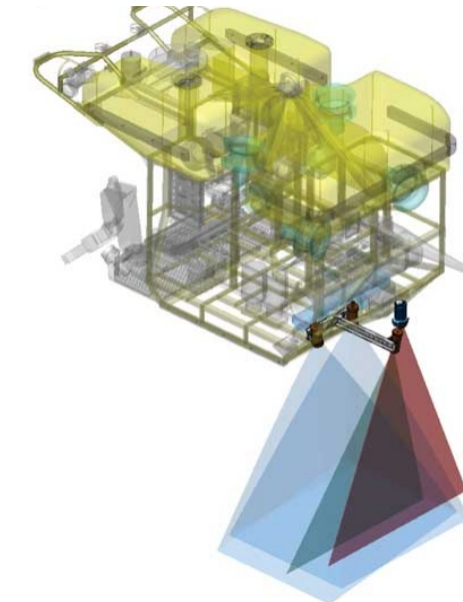
Random [bin picking](#) of 10-30 parts/minute (with surface inspection) with a 6R industrial robot, two pairs of cameras and a structured light sensor [Universal Robotics]



Structured light approach to best fit and [finish car bodies](#) (down to 0.1 mm) for reducing wind noise [Ford Motor Co.]



[Virtobot](#) system for post-mortem 3D optical scanning of human body & image-guided needle placement [Univ. Zürich]



[Hercules ROV](#) + structured-laser-light imaging system for high-resolution bathymetric underwater maps [Univ. Rhode Island]

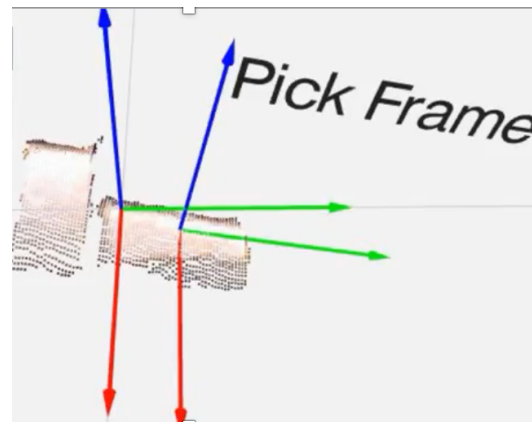
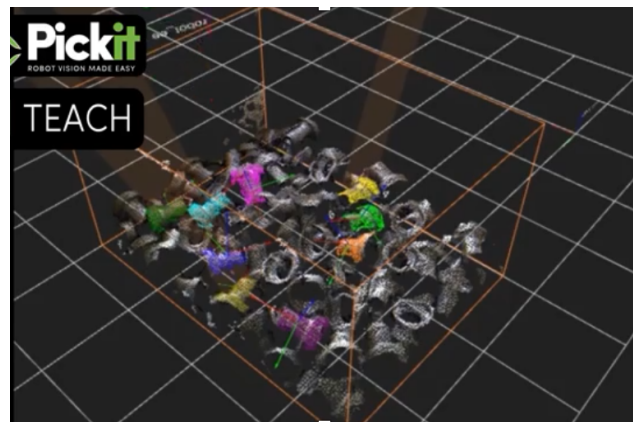
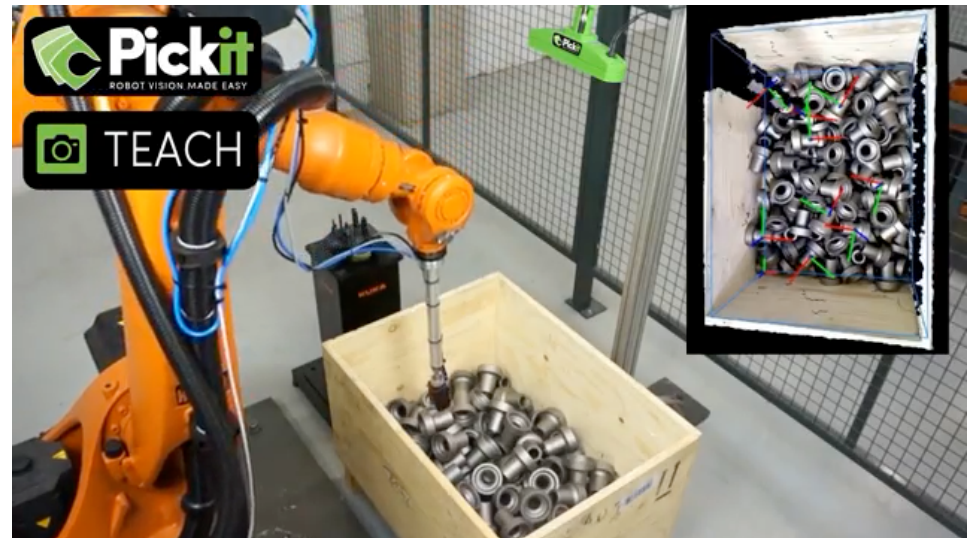


Robotic bin picking using vision (and structured light)

video

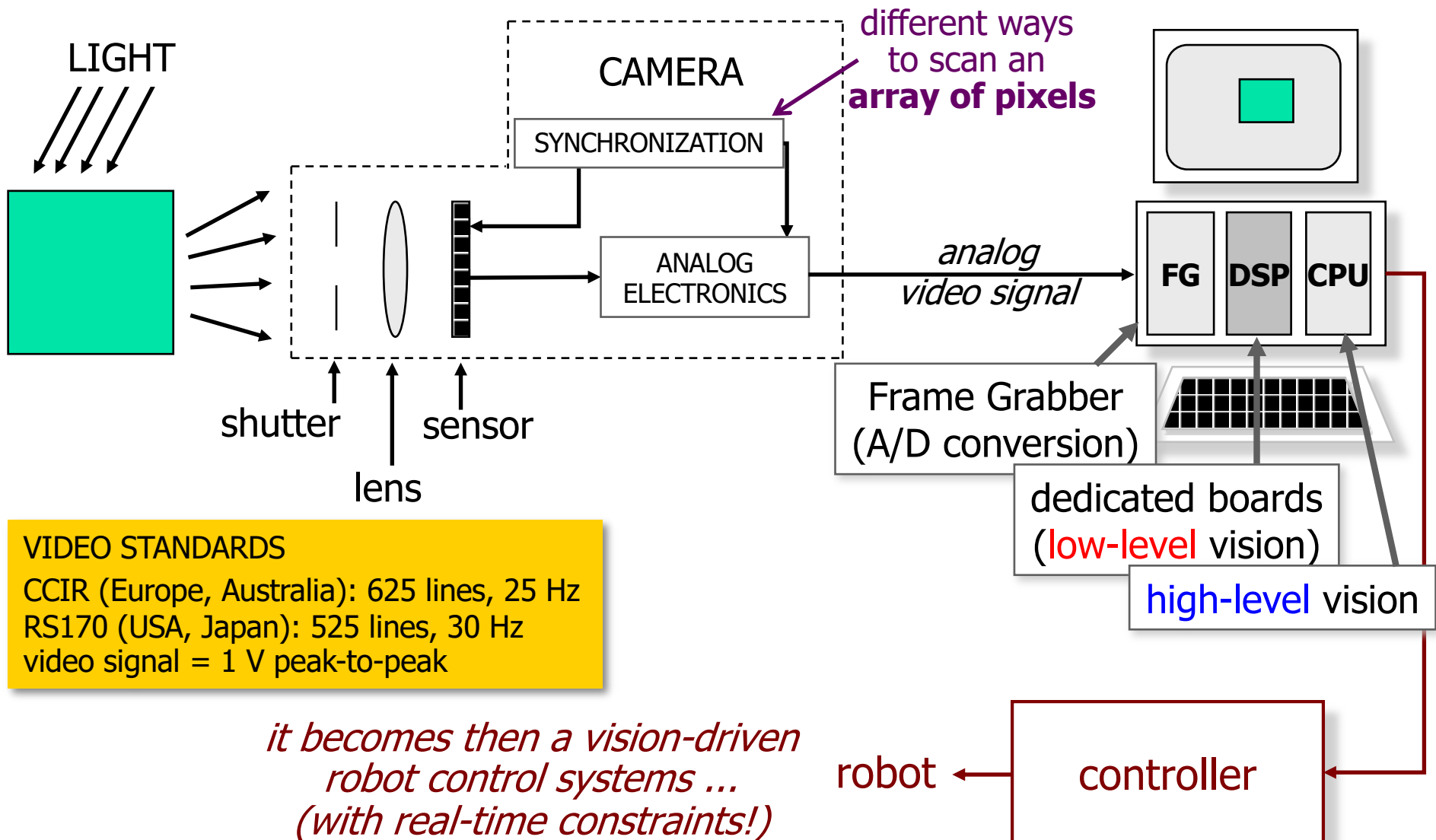


video





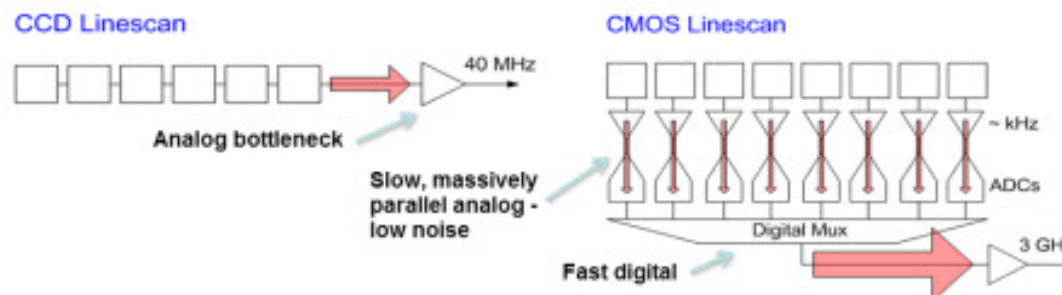
Vision systems





Sensors for vision

- arrays (spatial sampling) of photosensitive elements (**pixel**) converting light energy into electrical energy
- **CCD** (Charge Coupled Device): each pixel surface is made by a semiconductor device, **accumulating** free charge when hit by photons (**photoelectric effect**); “integrated” charges “read-out” by a sequential process (external circuitry) and transformed into voltage levels
- **CMOS** (Complementary Metal Oxide Semiconductor): each pixel is a **photodiode**, directly providing a voltage or current proportional to the **instantaneous** light intensity, with possibility of random access to each pixel





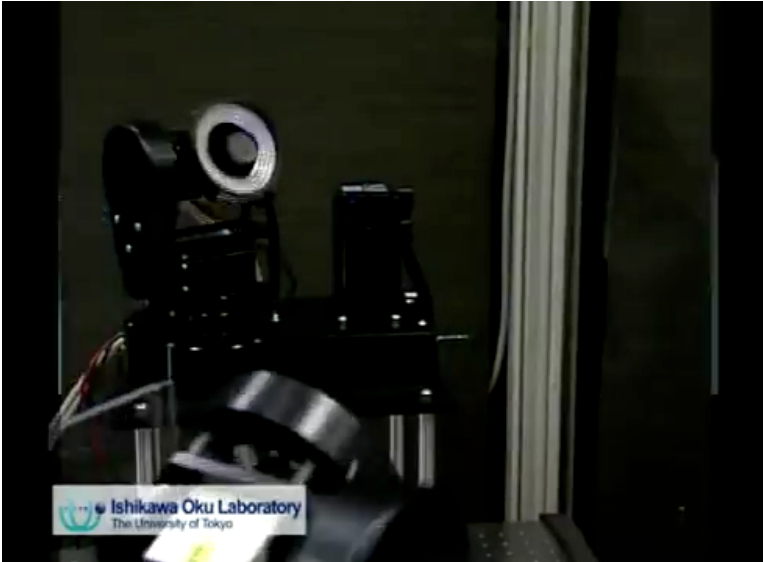
CMOS versus CCD

- reduction of fabrication costs of CMOS imagers
- better spatial resolution of elementary sensors
 - CMOS: 1M pixel, CCD: 768×576 pixel
- faster processing speed
 - 1000 vs. 25 fps (frames per second)
- possibility of integrating “intelligent” functions on single chip
 - sensor + frame grabber + low-level vision
- random access to each pixel or area
 - flexible handling of ROI (Region Of Interest)
- possibly lower image quality w.r.t. CCD imagers
 - sensitivity, especially for applications with low S/N signals
- customization for small volumes is more expensive
 - CCD cameras have been since much longer time on the market



Fast image processing for fast control

video



video



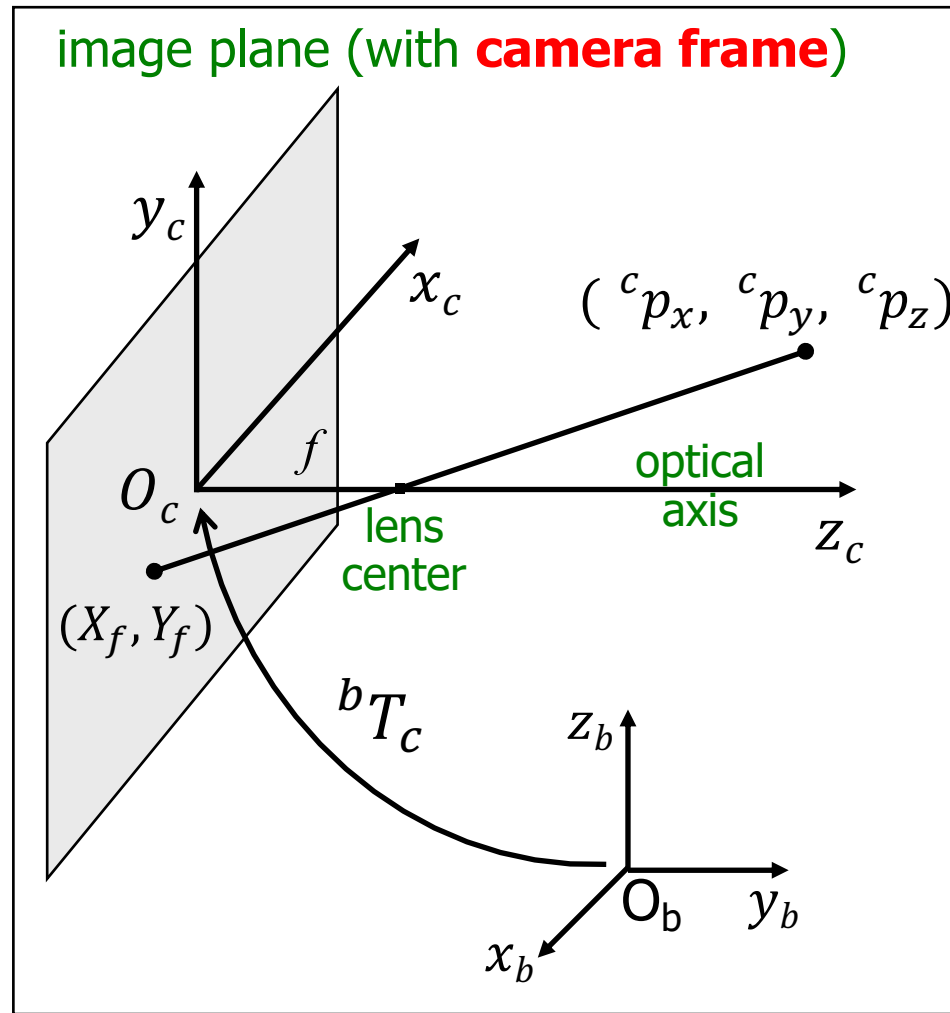
- 1 KHz vision frame rate
- 1 KHz robot control rate
@ Ishikawa Lab – U Tokyo
(2007-09)



video



Perspective transformation with pinhole camera model



1. in metric units

$$X_f = \frac{f \ {}^c p_x}{f - {}^c p_z} \quad Y_f = \frac{f \ {}^c p_y}{f - {}^c p_z}$$

2. in pixel

$$X_I = \frac{\alpha_x f \ {}^c p_x}{f - {}^c p_z} + X_0$$

offsets of pixel coordinate system w.r.t. optical axis

$$Y_I = \frac{\alpha_y f \ {}^c p_y}{f - {}^c p_z} + Y_0$$

pixel/metric scaling factor

3. LINEAR MAP in homogeneous coordinates

$$X_I = \frac{x_I}{z_I} \quad Y_I = \frac{y_I}{z_I} \quad \rightarrow \quad \begin{bmatrix} x_I \\ y_I \\ z_I \end{bmatrix} = \Omega \begin{bmatrix} {}^c p_x \\ {}^c p_y \\ {}^c p_z \\ 1 \end{bmatrix}$$

$$\Omega = \begin{bmatrix} \alpha_x & 0 & X_0 \\ 0 & \alpha_y & Y_0 \\ 0 & 0 & 1 \end{bmatrix} \begin{bmatrix} 1 & 0 & 0 & 0 \\ 0 & 1 & 0 & 0 \\ 0 & 0 & -1/f & 1 \\ 0 & 0 & 0 & 1 \end{bmatrix}$$

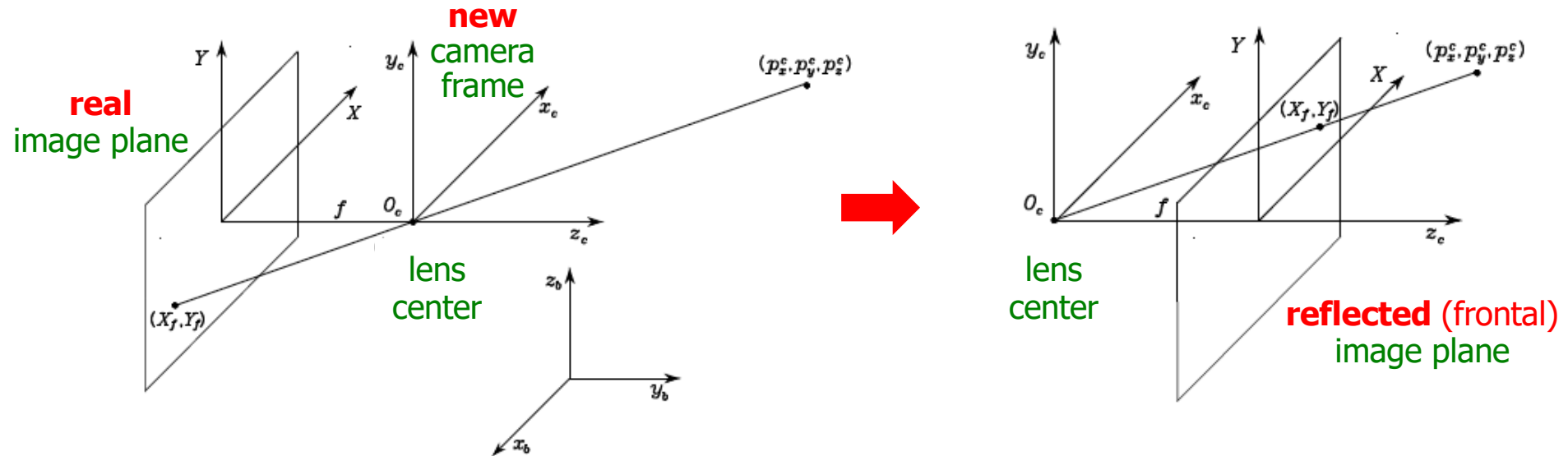
calibration matrix

$$H = \Omega \cdot {}^c T_b$$

intrinsic and extrinsic parameters



Perspective transformation with camera frame at the lens center



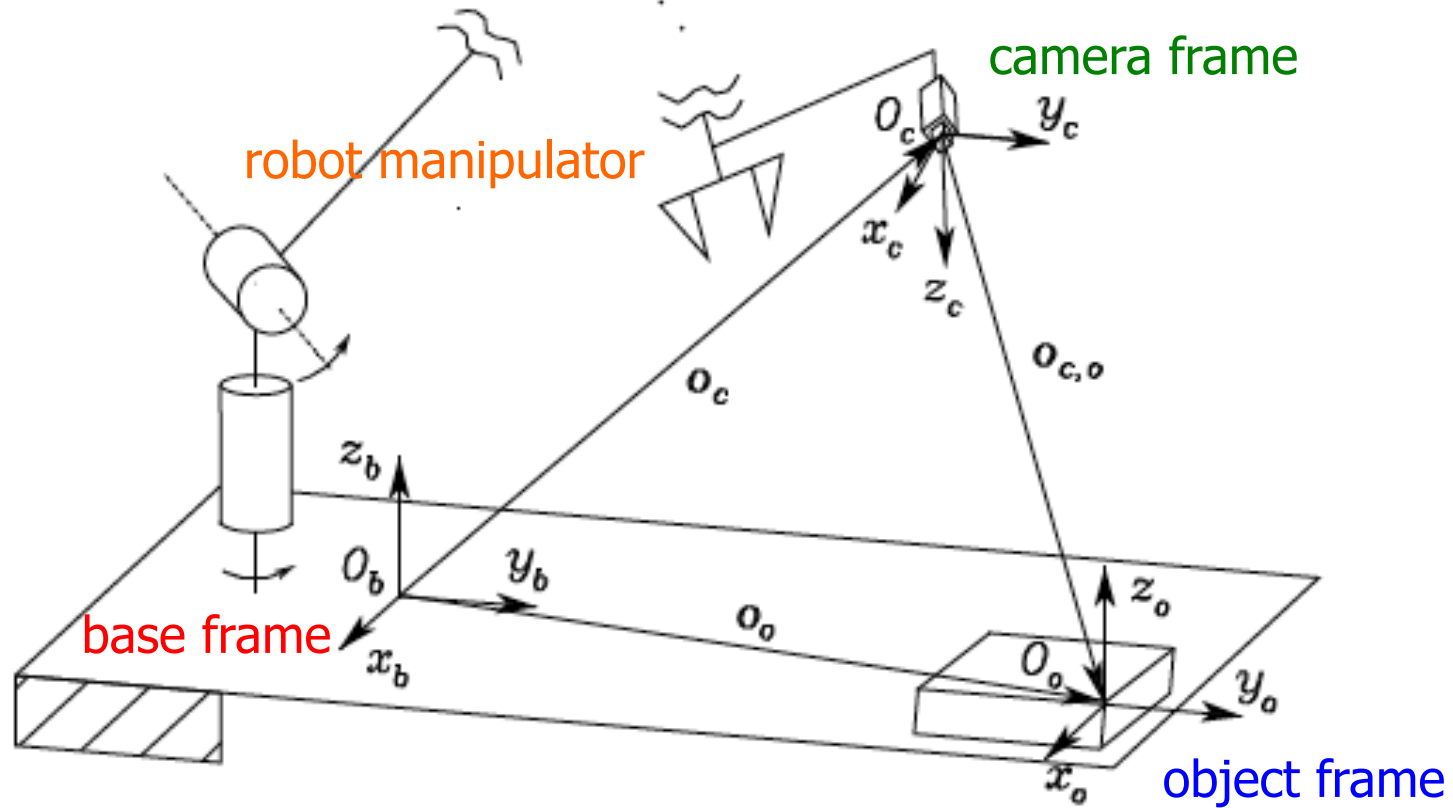
1. in metric units $X_f = -\frac{f}{c} \frac{p_x}{p_z}$ $Y_f = -\frac{f}{c} \frac{p_y}{p_z}$ \rightarrow $X_f = -\frac{f}{c} \frac{p_x}{p_z}$ $Y_f = -\frac{f}{c} \frac{p_y}{p_z}$

2. in pixel \dots \rightarrow $X_I = -\frac{\alpha_x f}{c} \frac{p_x}{p_z} + X_0$ $Y_I = -\frac{\alpha_y f}{c} \frac{p_y}{p_z} + Y_0$

3. LINEAR MAP in homogeneous coordinates \dots \rightarrow $\begin{bmatrix} x_I \\ y_I \\ z_I \\ 1 \end{bmatrix} = \Omega \begin{bmatrix} p_x \\ p_y \\ p_z \\ 1 \end{bmatrix}$ $\Omega = \begin{bmatrix} \alpha_x f & 0 & X_0 & 0 \\ 0 & \alpha_y f & Y_0 & 0 \\ 0 & 0 & 1 & 0 \end{bmatrix}$



Eye-in-hand camera



Relevant reference frames for visual-based tasks

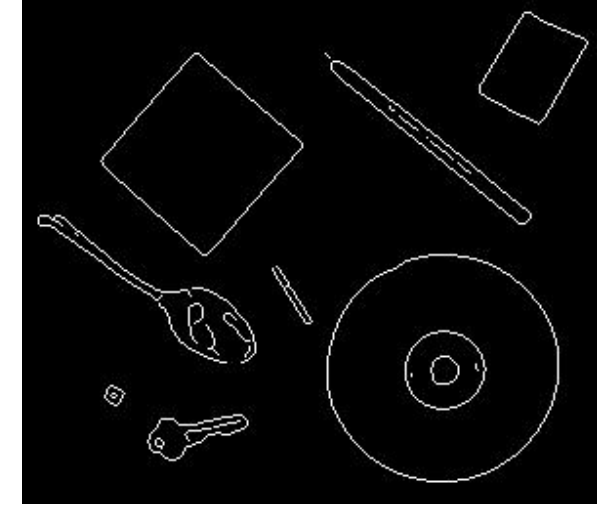


Low-level vision

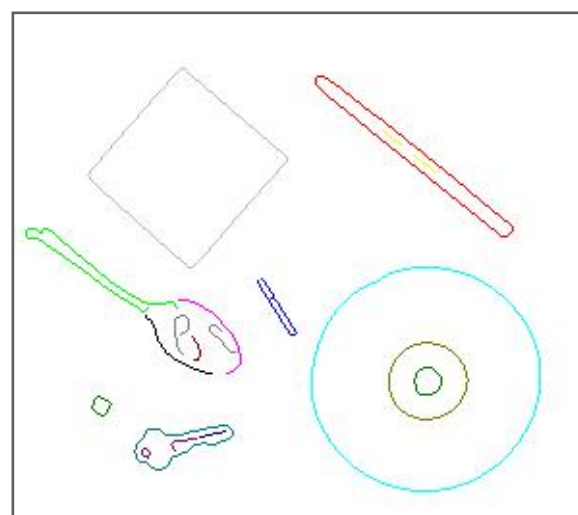
contour reconstruction



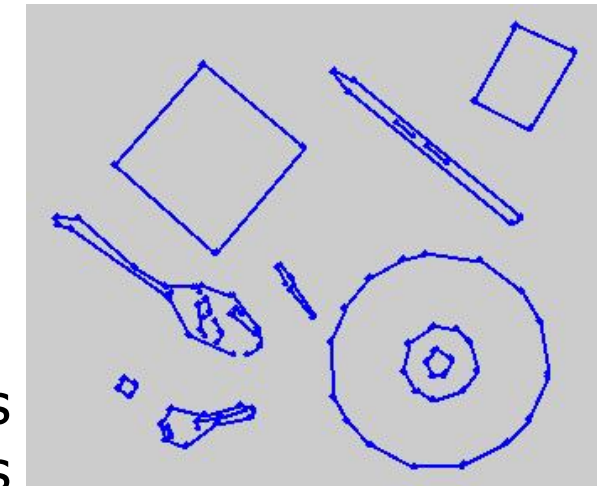
original image



edge detection



adjacent pixels on
the edges are
connected
and labeled with
different colors



linear segments
fitted to the edges



High-level vision

features matching in stereovision

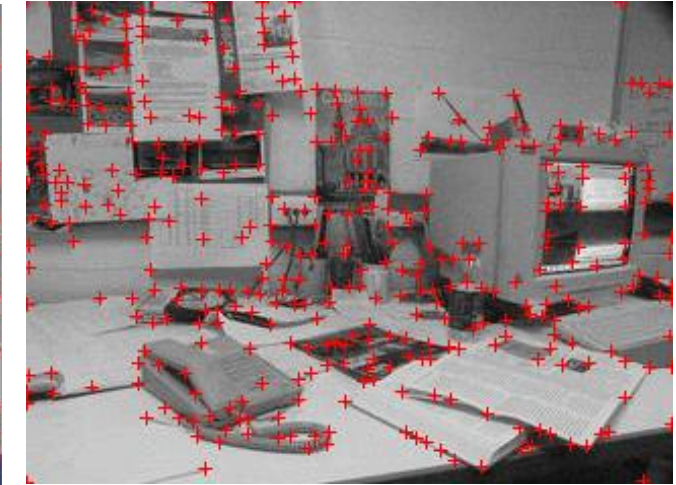
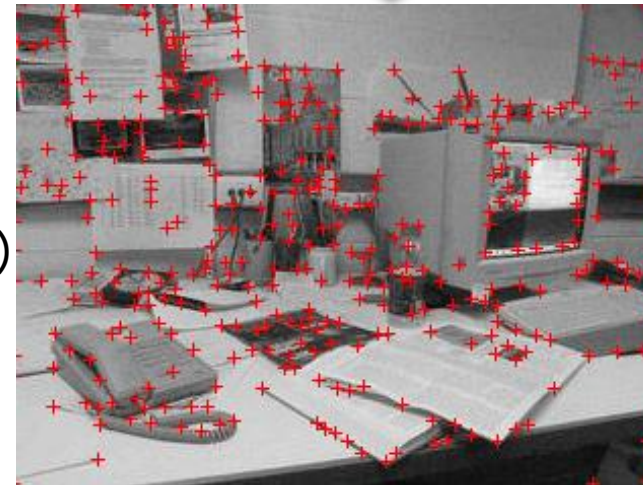


goal: find the
“fundamental matrix”
(rigid transformation
between the two images)
use: visual localization



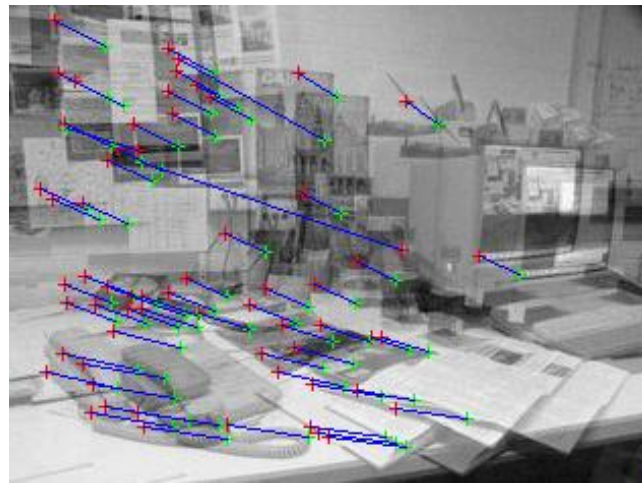
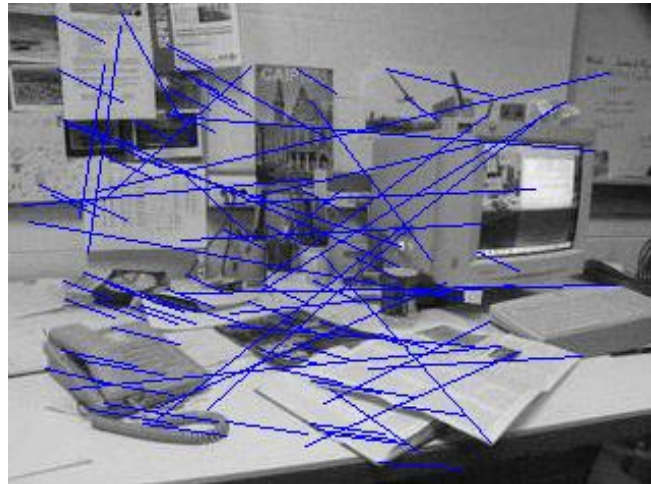
L- and R-views acquired, e.g.,
by stereocamera **Videre** ($\approx 5\text{cm}$)

corners in the two images
(in general, “features”)



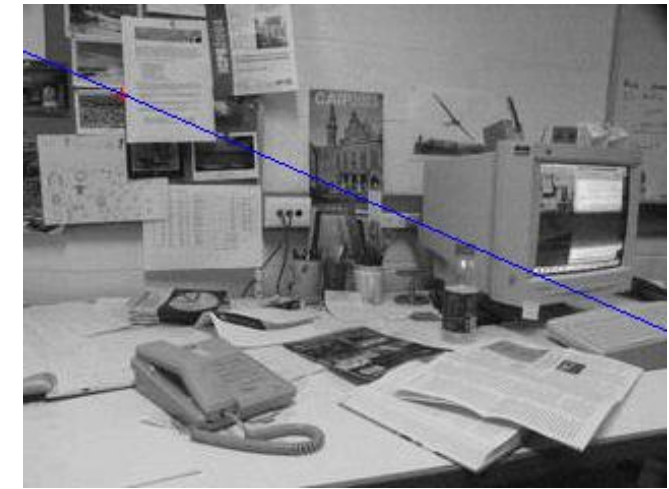
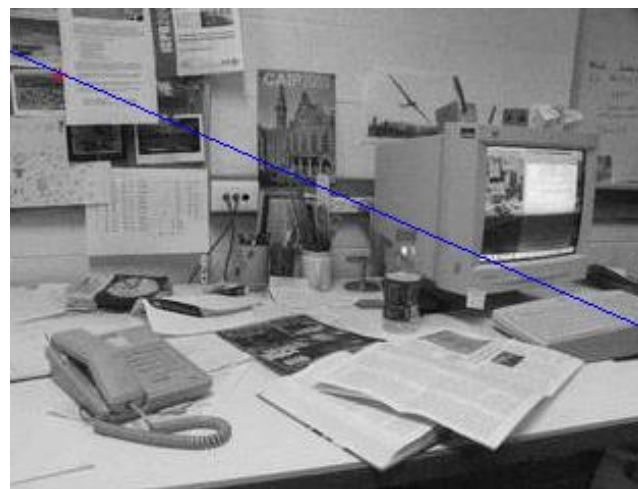


High-level vision (cont)



left: correspondence hypotheses used to find the best fitting fundamental matrix
right: inconsistent correspondences are eliminated

corresponding line
in the two images



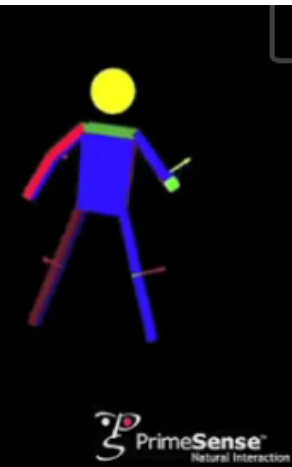


Kinect

camera + structured light 3D sensor



- RGB camera (with 640×480 pixel)
- depth sensor (by PrimeSense)
 - infrared laser emitter
 - infrared camera (with 320×240 pixel)
- 30 fps data rate
- range: $0.5 \div 5$ m
- depth resolution: 1cm@2m; 7cm@5m
- cost: < 90 €

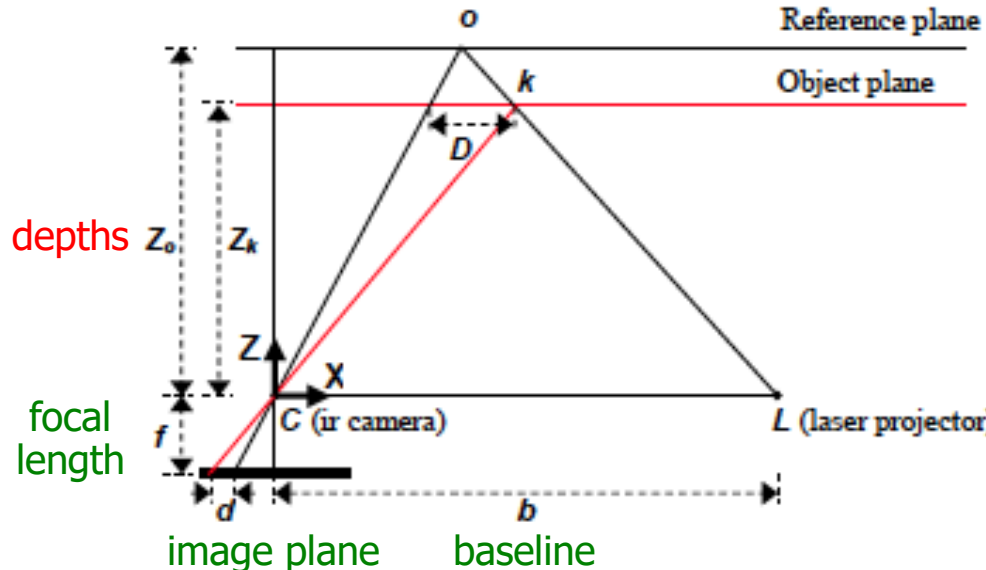


“skeleton” extraction and
human motion tracking



Kinect

Depth sensor operation



- stereo triangulation based on IR source emitting *pseudo-random* patterns
- reference pattern on IR camera image plane acquired in advance from a plane at known **distance** and coded in H/W
- correlating the disparity ***d*** (10 bits) of reference and received object patterns provides the **object depth *z_k***

1. **triangulation** equations (by similarity of triangles)

$$\frac{D}{b} = \frac{z_0 - z_k}{z_0} + \frac{d}{f} = \frac{D}{z_k} \rightarrow z_k = \frac{z_0}{1 + \frac{d}{fb} z_0} \quad \begin{matrix} \xrightarrow{\text{green}} x_k = -\frac{z_k}{f} (X_k - X_0 + \delta X) \\ \xrightarrow{\text{green}} y_k = -\frac{z_k}{f} (Y_k - Y_0 + \delta Y) \end{matrix}$$

2. accurate **calibration** of sensor

baseline length ***b***, depth of reference ***z₀*** + camera **intrinsic** parameters
(focal length ***f***, lens distortion coefficients ***δX, δY***, center offsets ***X₀, Y₀***)



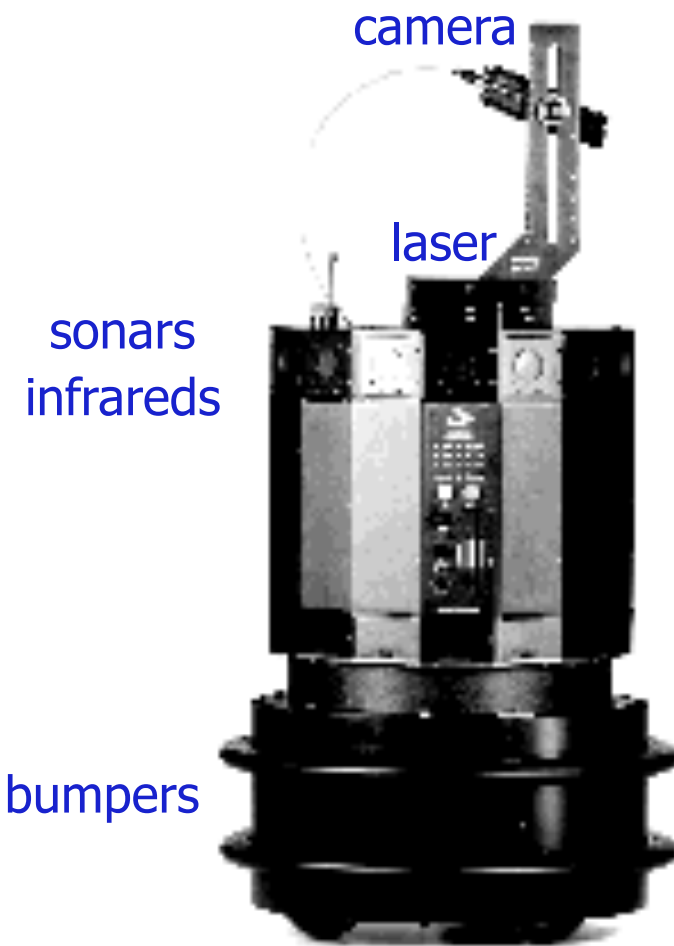
How Kinect works (a 2-minute illustration...)



<http://youtu.be/uq9SEJxZiUg>



Nomad 200 mobile robot



- structured light vision system (laser + CCD camera)
 - 480 scan lines/frame, 30 fps
 - range: 45÷300 cm
- 16 sonar sensors (Polaroid 50 KHz)
 - each with a field of view of 25°
 - range: 40÷640 cm, resolution 1%
- 16 infrared sensors
 - range: ≤ 60 cm, readings every 2.5 msec
- 20 pressure-sensitive bumpers
- radio-ethernet communication



Magellan Pro mobile robot

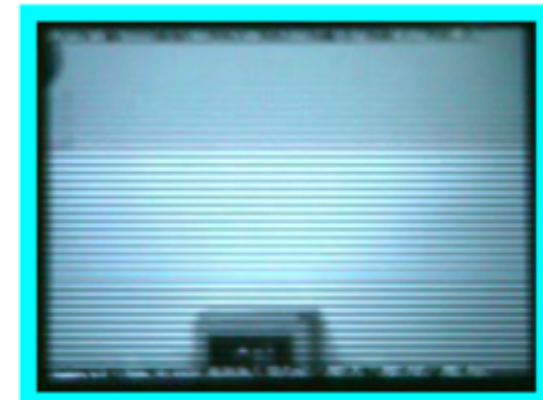
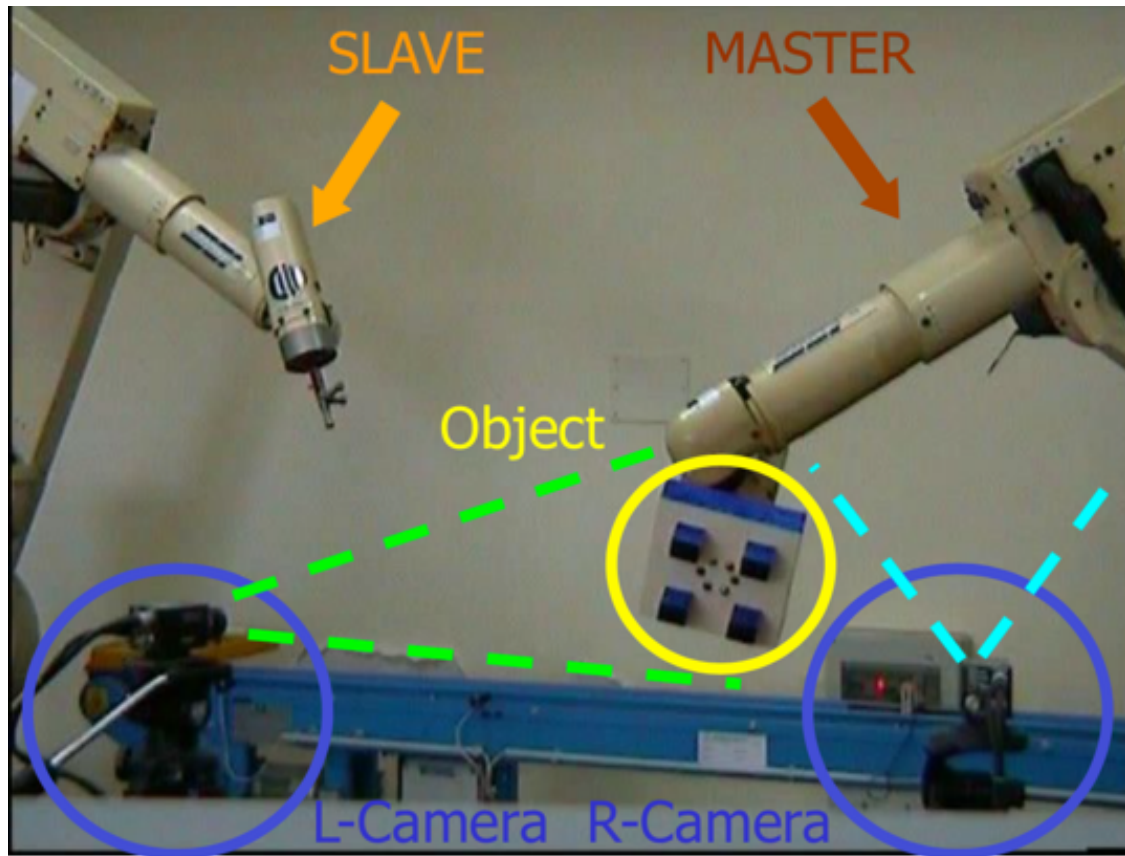


- pan-tilt color camera (7 Hz...)
- 16 sonar sensors
- 16 infrared sensors
- 16 pressure-sensitive bumpers
- ethernet radio-link



Manipulators and vision systems

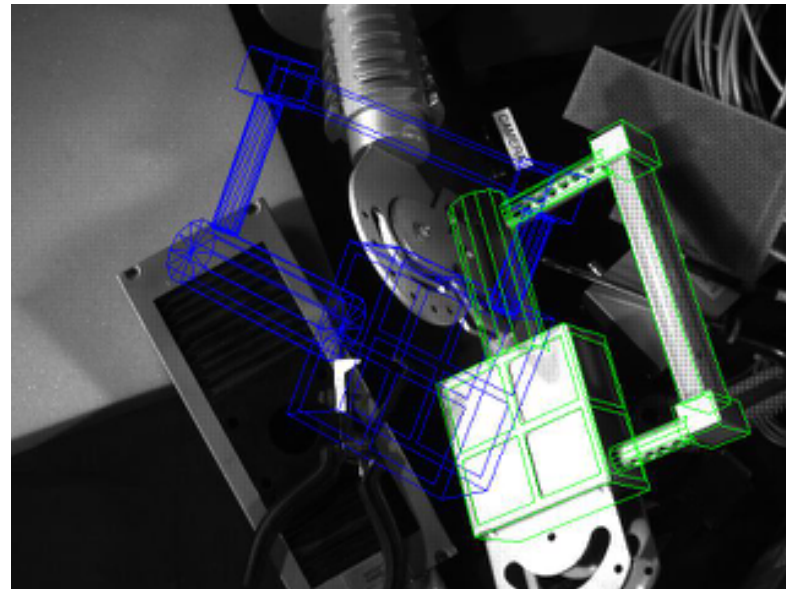
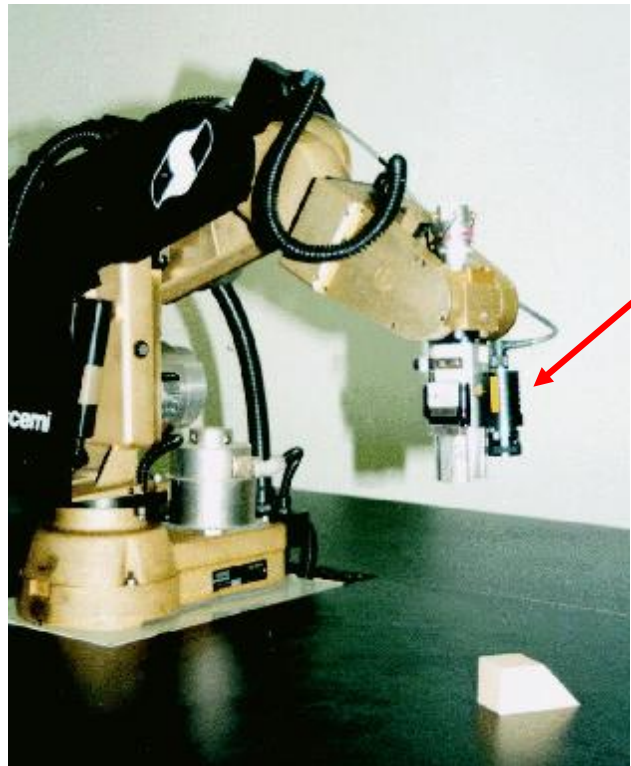
- stereovision with two external cameras, fixed in the environment (**eye-to-hand**)





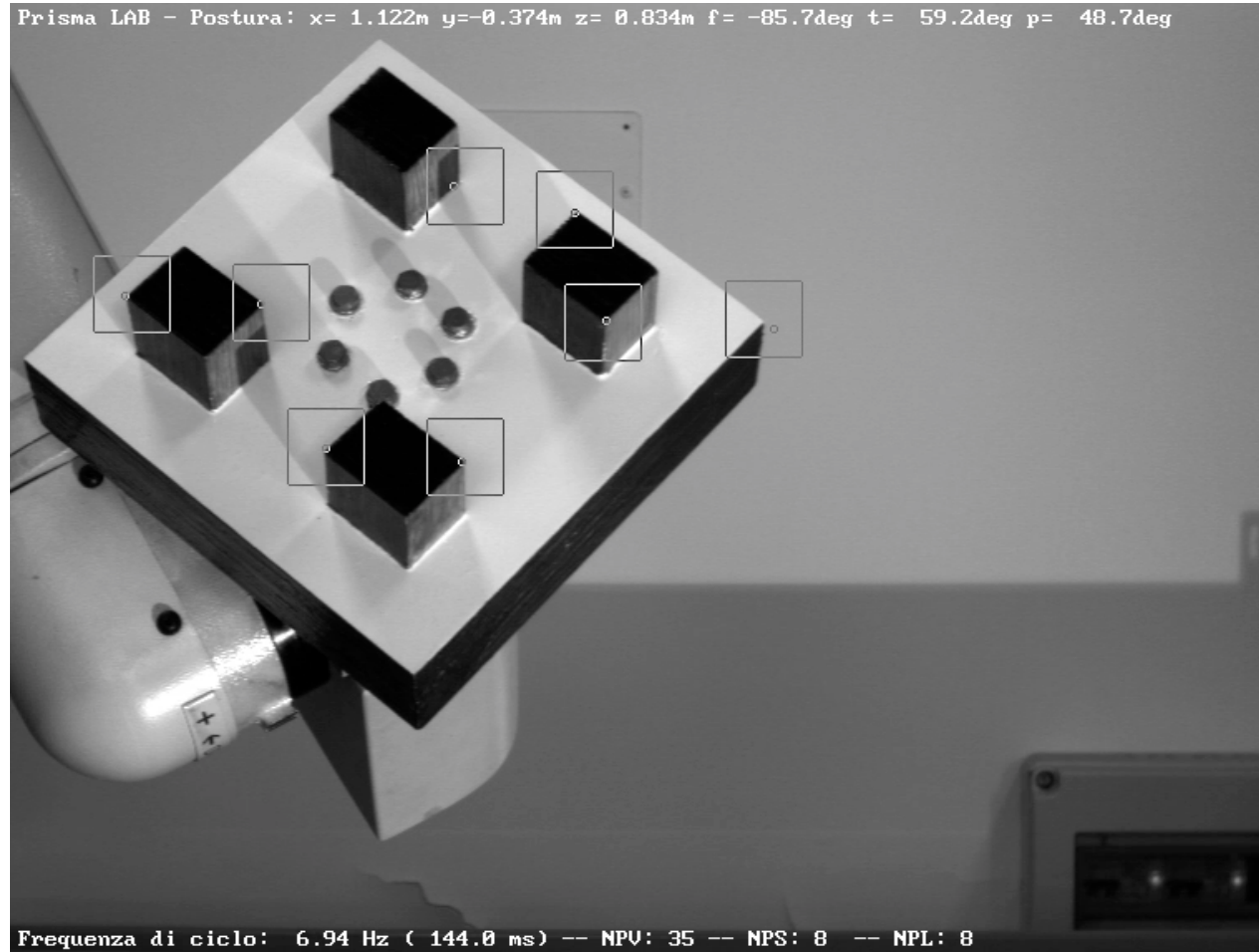
Manipulators and vision systems

- CCD camera mounted on the robot for controlling the end-effector positioning (**eye-in-hand**)





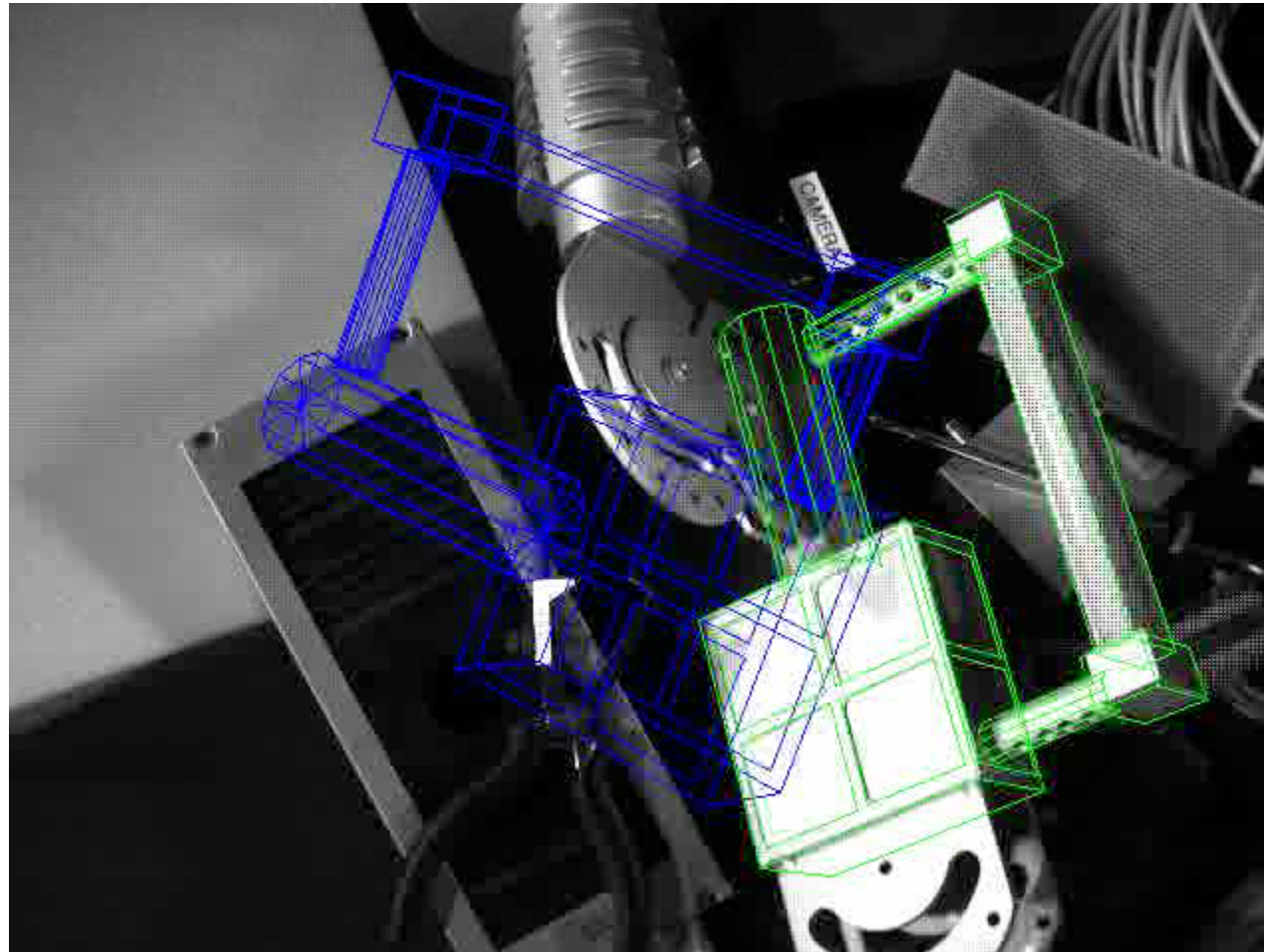
Visual tracking eye-to-hand



COMAU robot with position-based 6D tracking from external camera
(DIS, Università di Napoli Federico II)



Visual servoing eye-in-hand

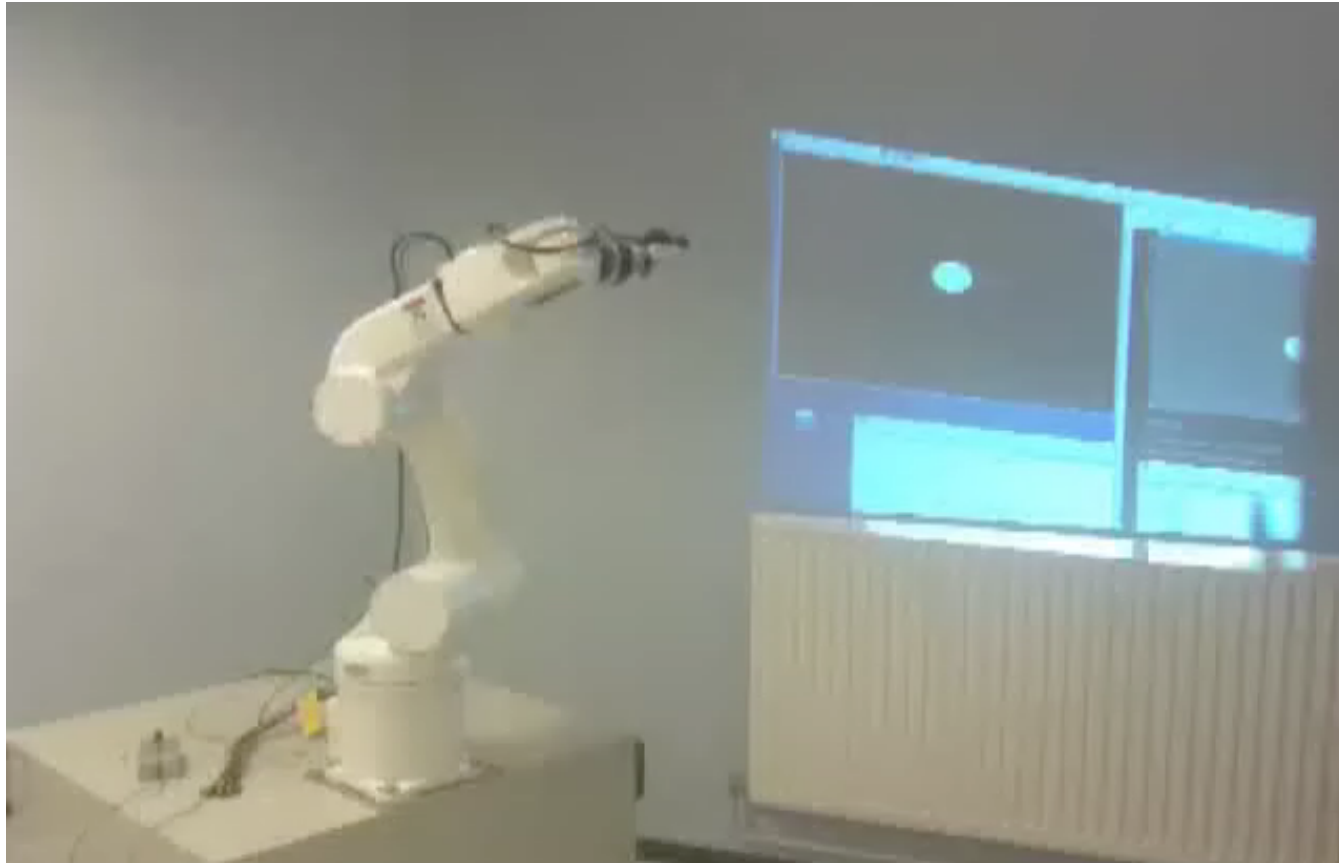


video

Image-based servoing with camera mounted on the robot end-effector
(IRISA/INRIA, Rennes)



Visual servoing and redundancy



[video](#)

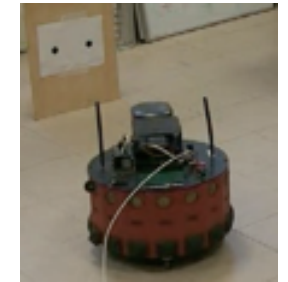
Visual servoing of circle feature ($m = 3: p_x, p_y, r$) by Adept Viper robot ($n = 6$):
redundancy is used for avoiding joint range limits (IRISA/INRIA, Rennes)



Visual servoing with mobile robot

video

pan/tilt (2 dof)
web cam at 7Hz
frame rate



Video attachment to ICRA'08 paper

Visual Servoing with Exploitation of Redundancy:
An Experimental Study

A. De Luca

M. Ferri

G. Oriolo

P. Robuffo Giordano

Dipartimento di Informatica e Sistemistica
Università di Roma "La Sapienza"

On-board image-based visual servoing with Magellan mobile robot
(DIS Robotics Laboratory, IEEE ICRA'08)



Combined visual/force assembly

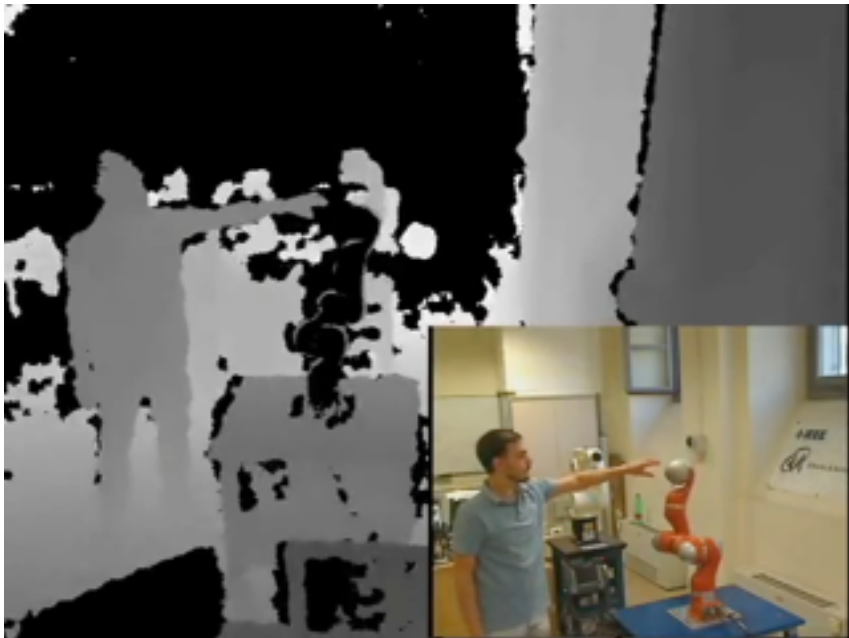


KUKA LWR with eye-in-hand camera and F/T sensor
(DLR, IEEE ICRA'07 demo in Roma)

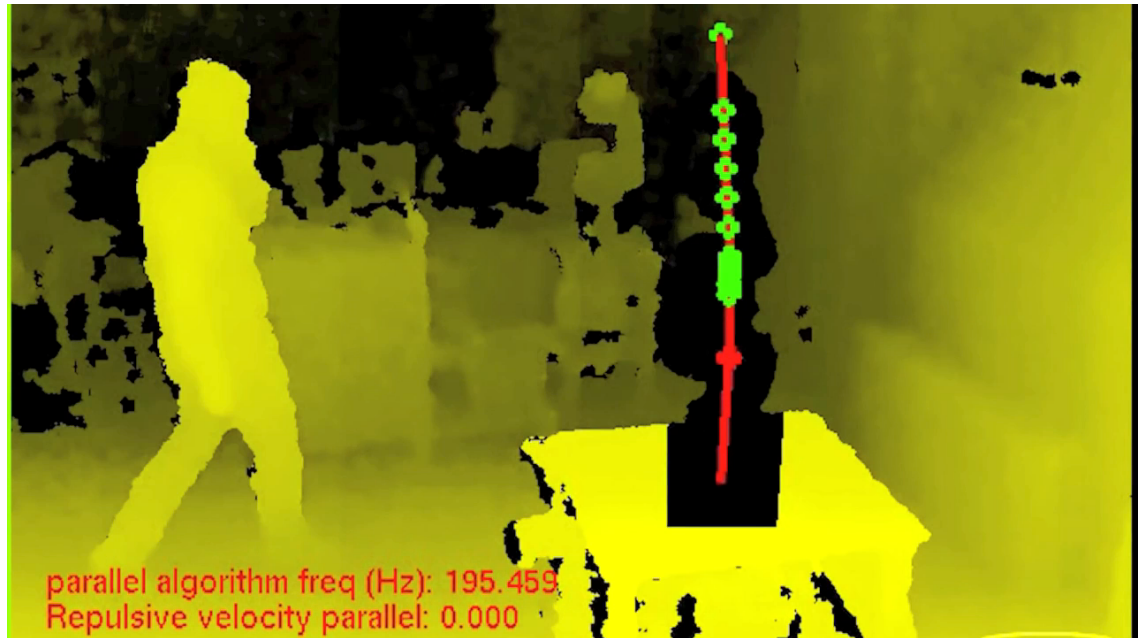
On-line distance computation and human-robot coexistence



video



monitoring **left-** and **right-hand**
distance to the robot (at same time)



several **control points** on robot **skeleton**
used to compute distances and control motion

KUKA LWR with a Kinect monitoring its workspace
(DIAG Robotics Laboratory, EU project SAPHARI, 2013)